November 2010

Environmental Technology Verification Report

VJ TECHNOLOGIES
IXS HIGH FREQUENCY
INTEGRATED X-RAY GENERATOR
ALTERNATIVE TECHNOLOGY FOR SEALED SOURCE RADIOGRAPHY CAMERAS

Prepared by
Battelle

Battelle
The Business of Innovation

Under a cooperative agreement with

EPA **U.S. Environmental Protection Agency**

November 2010

Environmental Technology Verification Report

ETV Advanced Monitoring Systems Center

VJ TECHNOLOGIES
IXS HIGH FREQUENCY
INTEGRATED X-RAY GENERATOR
ALTERNATIVE TECHNOLOGY FOR SEALED SOURCE RADIOGRAPHY CAMERAS

by

Stephanie Buehler, Bruce Nestleroth, Karen Riggs, and Amy Dindal, Battelle

John McKernan and Madeleine Nawar, U.S. EPA

Notice

Funding for this verification test was provided under Contract No. GS-23F-0011L-3, Task Order 1145, National Homeland Security Research Center, US Environmental Protection Agency (EPA). The U.S. EPA, through its Office of Research and Development, managed the research described herein. It has been subjected to the Agency's peer and administrative review. Any opinions expressed in this report are those of the author(s) and do not necessarily reflect the views of the Agency, therefore, no official endorsement should be inferred. Any mention of trade names or commercial products does not constitute endorsement or recommendation for use.

Foreword

The EPA is charged by Congress with protecting the nation's air, water, and land resources. Under a mandate of national environmental laws, the Agency strives to formulate and implement actions leading to a compatible balance between human activities and the ability of natural systems to support and nurture life. To meet this mandate, the EPA's Office of Research and Development provides data and science support that can be used to solve environmental problems and to build the scientific knowledge base needed to manage our ecological resources wisely, to understand how pollutants affect our health, and to prevent or reduce environmental risks.

The Environmental Technology Verification (ETV) Program has been established by the EPA to verify the performance characteristics of innovative environmental technology across all media and to report this objective information to permitters, buyers, and users of the technology, thus substantially accelerating the entrance of new environmental technologies into the marketplace. Verification organizations oversee and report verification activities based on testing and quality assurance protocols developed with input from major stakeholders and customer groups associated with the technology area. ETV consists of six environmental technology centers. Information about each of these centers can be found on the Internet at http://www.epa.gov/etv/.

Effective verifications of monitoring technologies are needed to assess environmental quality and to supply cost and performance data to select the most appropriate technology for that assessment. Under a cooperative agreement, Battelle has received EPA funding to plan, coordinate, and conduct such verification tests for "Advanced Monitoring Systems for Air, Water, and Soil" and report the results to the community at large. Information concerning this specific environmental technology area can be found on the Internet at http://www.epa.gov/etv/centers/center1.html.

Acknowledgments

The authors wish to acknowledge the support of all those who helped plan and conduct the verification test, analyze the data, and prepare this report. We also would like to thank Terry Webb, BP; Temeka Taplin, U.S. Department of Energy; and Mike Eagle, U.S. EPA for their careful review of the test/quality assurance plan and this verification report. Quality assurance (QA) oversight was provided by Michelle Henderson, U.S. EPA, and Zachary Willenberg and Rosanna Buhl, Battelle.

Contents

Figures

Tables

List of Abbreviations

ADE	Advanced Defect Enhancement
AMS	Advanced Monitoring Systems
API	American Petroleum Institute
ASNT	American Society for Nondestructive Testing
ATI	Alternative Technologies Initiative
DQI	data quality indicator
EPA	U.S. Environmental Protection Agency
ESH&Q	Environment, Safety, Health, and Quality
ETV	Environmental Technology Verification
GE	General Electric
HV	high voltage
IAEA	International Atomic Energy Agency
IQI	image quality indicator
IRRSP	Industrial Radiography Radiation Safety Personnel
kV	kilovolt
mA	milliamp
mm	millimeter
NDT	non-destructive testing
OAR	Office of Air and Radiation
PE	performance evaluation
QA	quality assurance
QC	quality control
QMP	Quality Management Plan
SOP	Standard Operating Procedure
TSA	technical systems audit
VMI	Virtual Media Integration

Chapter 1
Background

The U.S. Environmental Protection Agency (EPA) supports the Environmental Technology Verification Program (ETV) to facilitate the deployment of innovative environmental technologies through performance verification and dissemination of information. The goal of the ETV Program is to further environmental protection by accelerating the acceptance and use of improved and cost-effective technologies. ETV seeks to achieve this goal by providing high-quality, peer-reviewed data on technology performance to those involved in the design, distribution, financing, permitting, purchase, and use of environmental technologies.

ETV works in partnership with recognized testing organizations; with stakeholder groups consisting of buyers, vendor organizations, and permitters; and with the full participation of individual technology developers. The Program evaluates the performance of innovative technologies by developing test plans that are responsive to the needs of stakeholders, conducting field or laboratory tests (as appropriate), collecting and analyzing data, and preparing peer-reviewed reports. All evaluations are conducted in accordance with rigorous quality assurance (QA) protocols to ensure that data of known and adequate quality are generated and that the results are defensible.

The EPA's National Risk Management Research Laboratory (NRMRL) and its verification organization partner, Battelle, operate the Advanced Monitoring Systems (AMS) Center under ETV. The AMS Center recently evaluated the performance of the VJ Technologies IXS High Frequency Integrated X-Ray Generator for determining the ability of x-ray technologies to determine defects in pipeline, particularly to adequately identify defects through insulation to provide an alternative for radiography cameras.

Chapter 2
Technology Description

The objective of the ETV AMS Center is to verify the performance characteristics of environmental monitoring, sampling, characterization, and detection technologies. This report provides results for the verification testing of the VJ Technologies IXS High Frequency Integrated X-Ray Generator. The following is a description of the VJ Technologies IXS High Frequency Integrated X-Ray Generator, based on information provided by the vendor; this information was not verified.

The IXS technology (see Figure 2-1) is a compact, portable x-ray generator. It integrates a high-voltage (HV) power supply, an x-ray tube, and a filament supply into one single module. The design features a high-frequency inverter for compact design, power factor correction to minimize input power requirements, self-cooling to improve reliability and prolong product life, and radiation self-containment to ensure low x-ray leakage.

Figure 2-1. VJ Technologies IXS High Frequency Integrated X-Ray Generator.

The product comes with a HV module connected to a control module. The control module is powered by 110 volt (V) or 220 V of alternating current. The control interface uses a RS232 cable between the control module and a computer via a graphic user interface. The digital interface provides the ability to program and monitor the output voltage and current, monitor any fault conditions, and operate the x-ray interlock.

The IXS series x-ray systems are designed to be used for a wide range of non-destructive testing (NDT) applications including: industrial radiography, baggage security inspection, medical radiography and fluoroscopy, food and package inspection, and electronic component inspection. The product offers a platform with output power ranging from 10 kilovolts (kV) to 160 kV, and up to 500 watts (W) continuously, with higher power available for x-ray pulsing applications. Its modular design allows customization of beam shapes (cone or fan), focal spot sizes (0.05 millimeters [mm] to 1.5 mm), and mounting methods.

The IXS High Frequency Integrated X-Ray Generator is 16 inches long by 5.6 inches wide by 15 inches high. It weighs 59 pounds. The list price for a 500 W (160 kilovolts @ 3.12 milliamp [mA]) model is $15,000. A computer, imaging plates, and image processing equipment are not included with the unit, and must be purchased separately.

Chapter 3
Test Design and Procedures

3.1 Introduction

Radioactive materials, such as sealed sources of Cobalt-60, Cesium-137, Selenium-75, and Iridium-192 oxides, are found in medical, commercial, and industrial devices such as those used for measuring material thickness. Minimizing the number of such radioactive sources in the public domain is more sustainable for the environment and would decrease opportunities for terrorists to obtain radioactive sources when inappropriately disposed.

As a major component of NDT, radiography cameras use gamma-rays to penetrate material and provide an image of hidden flaws. Radiography cameras employ film plates to record an image of the pipe or vessel being inspected. Generally, standard methods such as American Society of Testing Materials (ASTM) E 94[1], International Organization for Standardization ISO 5579[2], and the British Standard BS EN 444[3] provide guidelines to ensure safe and quality testing using radiography cameras. This test utilized ASTM E 94 to define image quality for the reference method. Iridium-192 and Cobalt-60 are the most common gamma radiation sources used. In addition to the significant safety concerns if sealed source radiation is mishandled or improperly disposed, use of these cameras calls for meeting specific licensing and regulation requirements and restricting access to large areas. The use of sourced alternative technologies, where applicable, could help to eliminate these health and safety concerns. These technologies include x-ray (pulsed or high voltage) sources.

The EPA's Office of Radiation and Indoor Air in the Office of Air and Radiation (OAR) established the EPA's Alternative Technologies Initiative (ATI). Part of the EPA ATI aims to foster the acceptance and voluntary market adoption of technologies; i.e., alternative technologies to those that currently use sealed radioactive sources. The EPA ATI is focusing primarily on alternative technologies for devices with Category 3 and 4 radioactive sources as classified by the International Atomic Energy Agency (IAEA). Commercial-ready or available alternatives to radiography cameras are being considered.

X-ray devices can be operated more safely than sealed-source radiography cameras because they do not contain radioactive sources and therefore operators do not have the same waste concerns. However, their ability to perform comparably to sealed-source radiography cameras in various situations is not well characterized. Although x-ray technologies have been used for decades, isotope-based radiography is still commonly used in oil refineries and petrochemical plants because the sources are generally easier to transport and position. One particular area of interest

in the capabilities of x-ray devices is their ability to detect pipeline defects through insulation. This verification test evaluated the ability of an x-ray technology to determine defects in pipeline similar to that found in an oil and gas industry refinery in comparison to a commonly used radiography camera with a Selenium-75 source. Testing was designed in particular to identify defects through pipeline insulation.

The VJ Technologies IXS High Frequency Integrated X-Ray Generator was verified by evaluating the following parameters.

- Detection of defects – qualitative results
- Detection of defects – quantitative results
  - Percent error
  - Percent difference
- Operational factors

Testing was conducted on June 1, 4, 5, and July 8, 2010 on subsections of two pipes at Battelle's Pipeline Facility in West Jefferson, Ohio, according to procedures specified in the *Test/QA Plan for Verification of Alternative Technologies for Sealed Source Radiography Cameras and Amendment 1 dated July 6, 2010*[4] and in compliance with the data quality requirements in the AMS Center Quality Management Plan (QMP).[5] As indicated in the test/QA plan, the testing conducted satisfied EPA QA Category II requirements. The test/QA plan and this verification report were reviewed by the following experts in the fields related to NDT pipeline inspections and alternatives to sealed-source technologies.

- Terry Webb, BP, Refining NDT Specialist
- Temeka Taplin, National Nuclear Security Administration, Department of Energy
- Mike Eagle, U.S. EPA

Two of these technical experts also came to the field site to observe testing. Verification testing was conducted by appropriately trained personnel following the safety and health guidelines for Battelle's Pipeline Facility, and following the guidance of Battelle's radiation safety officer.

The ability of the VJ Technologies IXS High Frequency Integrated X-Ray Generator to detect the defect was compared to the radiography camera's findings. Qualitative results of defect detection were determined by viewing the image(s) of the defect, and assessing if the technology did indeed discover a defect of appropriate size and shape in the appointed area. These results were then compared to those from the radiography camera. A number of images were also compared qualitatively by dividing the area of interest (i.e., weld and natural corrosion) into 10 zones and discussing the detection of defects in those zones. The number and type of defects found by the x-ray technology were compared qualitatively to the number and type of defects found by the radiography camera.

As described in Chapters 5 and 6, quantitative results of defect detection were determined by performing percent error and percent difference calculations on measurements determined from images obtained by the radiography camera and the VJ Technologies IXS High Frequency Integrated X-Ray Generator. Percent error was calculated for the reference (i.e., radiography

camera) and x-ray technology by subtracting the actual physical measurement of the defect from the estimated measurement, and normalizing the calculation to the wall thickness of the pipe. Percent difference was assessed by comparing the difference between the x-ray and radiography camera results. Operational factors and sustainability metrics were evaluated based on testing observations and input provided from the testing staff and the Verification Test Coordinator. These factors and metrics included maintenance needs, power needs, calibration frequency, data output, consumables used, ease of use, repair requirements, training and certification requirements, safety requirements, and image throughput.

3.2 Test Facility

Testing was conducted on June 1, 4, 5 and July 8, 2010 at Battelle's Pipeline Facility in West Jefferson, Ohio.

3.3 Test Procedures

Subsections of two pipes (see Figure 3-1) were examined by both the VJ Technologies IXS High Frequency Integrated X-Ray Generator and a radiography camera. These pipe samples were similar but not identical to pipes in a refinery, as the verification test pipes had similar diameter but thinner wall thickness. Refineries typically use four to 12-inch diameter pipes, and the pipe samples used were eight inches in diameter. The test was conducted outdoors in Battelle's pipe specimen storage yard. The pipe was placed about three feet off the ground on stands or timbers as shown in Figure 3-1.

Figure 3-1. Pipe Sample 1 (top, right) with insulation and Pipe Sample 2 (bottom, left).

Pipe Sample 1 was a seam-welded carbon steel pipe measuring approximately 35 feet in length. The wall thickness was 0.188 inches. This sample consisted of three pipe sections welded together (two circumferential welds) and contained simulated corrosion defects set along two test lines 180 degrees apart. A five foot section in the middle of Pipe Sample 1 also contained natural corrosion from a pipe pulled from service. The pipe sections with the simulated

corrosions were manufactured to American Petroleum Institute (API) specification X-52. The API grade of the pipe section with natural corrosion was not known.

To simulate the refinery environment, a portion of Pipe Sample 1 was insulated with calcium silicate material, a common industrial insulating material. The insulation was jacketed with aluminum sheet metal. The jackets were held on by aluminum banding material (see Figure 3-1).

While Pipe Sample 1 had over a dozen corrosion areas and three welds, a subset of the welds and corrosion was used to assess the x-ray technologies. The assessment included the following:

- Four simulated corrosion defects. Two images of each defect were collected with the x-ray beam oriented 90 degrees to the centerline of the pipe. One was to assess the length and width of the corrosion, and the other was to assess the length and depth.
- One weld. Two images were collected 90 degrees from the centerline.
- One natural corrosion area. Two images were collected 90 degrees from the centerline.

The natural corrosion was close to the weld, and both areas were assessed from the same image. Four simulated corrosion defects (P1-18, P1-7, P1-1, and P1-23), one natural corrosion defect (P1-9), and the weld next to the selected natural corrosion region were used. The test/QA plan[4] called for only three simulated corrosion defects to be used for this verification test. All three of these defects (P1-18, P1-7, and P1-23) were under the insulation that was placed on Pipe Sample 1. During testing, however, an additional simulated corrosion defect on Pipe Sample 1 that was not covered by insulation was imaged by both the VJ Technologies IXS High Frequency Integrated X-Ray Generator and the radiography camera. This was done to provide further information on the capabilities of the x-ray technology on exposed pipe corrosion. All areas of interest on Pipe Sample 1 were defined as 'patches'. Each patch on Pipe Sample 1 was a specific area of general corrosion with defined pits within it. Further details on this can be found in Appendix A.

Pipe Sample 2 was a stainless steel alloy of unknown composition measuring approximately 52 inches in length. The wall thickness was 0.515-inch. The surface was nominally in original condition. Since there were no corrosion anomalies, three holes of varying diameter and depth were drilled into the pipe using handheld tools to simulate pit defects. Two images were collected for the simulated defects on Pipe Sample 2 by the VJ Technologies IXS High Frequency Integrated X-Ray Generator and the radiography camera; One to assess the diameter of the drilled hole, and the other to assess the depth. In addition, a 'contact image' (i.e., the camera was placed in contact with the pipe) was collected for the simulated defects on Pipe Sample 2 by both the vendor and reference technology. The contact image was not called for in the test/QA plan[4] but was conducted to provide a comprehensive picture of the VJ Technologies IXS High Frequency Integrated X-Ray Generator performance.

The defects on both pipes were labeled alphabetically, and their location under the insulation was marked with a spot on the aluminum sheeting using a marker. This was done to ensure that the VJ Technologies IXS High Frequency Integrated X-Ray Generator and the reference technology were imaging the same location. This was not a test to see if the technologies could find the same area under the insulation, but how well they could detect the same defects under insulation.

The defects were evaluated in no particular order. Reference testing of these defects using a radiography camera was conducted prior to testing using the x-ray technology.

Testing was conducted outdoors on separate days for the radiography camera and the VJ Technologies IXS High Frequency Integrated X-Ray Generator. This allowed each technology operator ample time and space to set up and collect images with the devices. The VJ Technologies IXS High Frequency Integrated X-Ray Generator was operated by VJ Technologies and their representatives. The radiography camera was supplied and operated by Mistras, a local professional NDT company (Columbus, OH). Mistras employed a radiography camera with a QSA Global Selenium-75 spherical source with an activity of 41 Curies. This source was chosen by Mistras based on current NDT practices, and the needs of this test. Operation of the instruments, and the establishment of radiation safety boundaries were conducted by persons with an American Society for Nondestructive Testing (ASNT) Industrial Radiography Radiation Safety Personnel (IRRSP) certification.

Both Mistras (the radiography camera operator) and VJ Technologies collected analog images on General Electric (GE) phosphor imaging plates. After exposure, each imaging plate was placed into a computed radiography scanner where the image was retrieved using laser light scanning, and stored as a digital file. The corresponding images were assessed and evaluated by their respective operators (VJ Technologies for the x-ray technology images and Mistras for the radiography camera images) to determine specific characteristics of the defects used for analysis of the technology. Mistras also assessed and evaluated the VJ Technologies IXS High Frequency Integrated X-ray Generator images. Battelle technical staff members who specialize in NDT measurements also reviewed the images from both the VJ Technologies IXS High Frequency Integrated X-Ray Generator and the radiography camera used by Mistras to confirm the results.

The initial round of testing was performed in June 2010. During this testing, Mistras used a Virtual Media Integration (VMI) 5100 computed radiography scanner and associated StarrView 7 software to retrieve the image onsite from the phosphor imaging plates generated by the radiography camera. Images collected by the VJ Technologies IXS High Frequency Integrated X-Ray Generator were processed by VJ Technologies with an AllPro Imaging computed radiography scanner and GE Rhythm software. Using this processing equipment, the images collected by the VJ Technologies IXS High Frequency Integrated X-Ray Generator were not providing images of the defects. It was unclear if this result was related to the performance of the VJ Technologies IXS High Frequency Integrated X-Ray Generator, or a problem with the processing equipment and software. Therefore, images from the initial round of testing were not used for the performance evaluation of the VJ Technologies IXS High Frequency Integrated X-Ray Generator.

Re-testing was performed in July by the VJ Technologies IXS High Frequency Integrated X-Ray Generator with Mistras onsite to provide and process the phosphor imaging plates (GE imaging plates) using the same system (VMI 5100 computed radiography scanner and associated StarrView 7 software) used initially for the radiography camera. Because the radiography camera images could be interpreted, no additional images were collected using the radiography camera. The same VJ Technologies IXS High Frequency Integrated X-Ray Generator was used in both the June and July tests. As described in an amendment to the test/QA plan that was

requested by the EPA Quality Manager after the June testing, electronic image files were labeled with the date and approximate time the image was captured in July. Both Mistras and the vendor evaluated the images from the x-ray system and provided measurements for data analysis. Images collected during re-testing using the GE imaging plates and VMI 5100 computed radiography scanner and associated StarrView 7 software were readable and were used to evaluate the performance of the VJ Technologies IXS High Frequency Integrated X-Ray Generator. It is assumed that because images were obtained using the VJ Technologies IXS High Frequency Integrated X-Ray Generator and the Mistras image processing system, that there was a problem with the original image processing system used by VJ Technologies (AllPro scanner and Rhythm software), though this could not be independently verified. Discussions in the remainder of this report of the VJ Technologies IXS High Frequency Integrated X-Ray Generator performance refer to testing and results that occurred during the re-testing on July 8, 2010 using the VMI 5100 computed radiography scanner and associated StarrView 7 software with GE imaging plates.

3.3.1 Test Sample Preparation and Storage

The simulated corrosion in Pipe Sample 1 was created using electrochemical etching techniques. These areas of simulated corrosion were prepared prior to the development of this verification test, as Pipe Sample 1 has been used in other Battelle studies. The defects on Pipe Sample 1 were thoroughly characterized at the time of their creation. Appendix A provides detailed information on the characteristics of the defects on Pipe Sample 1 as determined during this previous characterization. The insulation on Pipe Sample 1 was installed professionally by a qualified local company, Sauer Group, Inc., Columbus, OH for this verification test.

Three simulated defects on Pipe Sample 2 were created using a drill. Each defect depth was measured using a Starrett 449 depth micrometer. Each defect diameter was measured using a Starrett 120 slide caliper. Measurement accuracy was within ± 10% of the wall thickness of Pipe Sample 2 (0.515 inch). Accuracy was measured to ± 0.002 inch. The actual diameter and depth of these defects are below.

- Pit 1: 0.375 inch diameter, 0.188 inch depth
- Pit 2: 0.313 inch diameter, 0.115 inch depth
- Pit 3: 0.252 inch diameter, 0.316 inch depth

3.3.2 Test Sample Analysis Procedure

The VJ Technologies IXS High Frequency Integrated X-Ray Generator was operated by a representative of VJ Technologies. Scanning of the phosphor imaging plates was conducted by a Mistras representative. A radiation safety area between 40 to 80 feet (technology dependent) was established, and entry to this area was restricted during the testing. The exposure time for the VJ Technologies IXS High Frequency Integrated X-Ray Generator was 1 minute. The x-ray generator was placed 28 inches away from the defect (except for the contact image) and was operated at 3 mA and 160 kV. The IXS High Frequency Integrated X-Ray Generator was either placed on a tripod stand for images through the diameter of the pipe, or on a forklift for images captured above the pipe. A one inch comparator ball shielded in lead, the same one as used by Mistras with the radiography camera, was taped to the pipe and used in each image. For the

contact image, an ASTM B wire pack as well as ASME 1025 stainless steel number 12, 15, and 17 plaque hole penatrameters were used to assess image quality. These image quality indicators were taped onto Pipe Sample 2 beside the visible defects. Lead markers ("0" and "1") were also used to note the direction of the images for all images. Mistras also used lead markers during the reference testing, and wrote the placement of these lead markers in permanent marker on the pipe. VJ Technologies then used the marks made by Mistras to ensure the images and placement of their plates was as close as possible to those collected by the reference technology. The images were collected on GE phosphor imaging plates and were scanned on-site using a VMI 5100 computed radiography scanner and associated StarrView 7 software. Initially, multiple images were collected for one defect until the right distance and exposure time were determined to obtain the best image quality for subsequent defect images. Only images that yielded the appropriate image quality, and where the lead comparator ball was clearly visible in the image, were used in assessing the defects.

3.4 Test Parameters

The performance of the VJ Technologies IXS High Frequency Integrated X-Ray Generator was verified based on the qualitative and quantitative detection of defects and operational factors, as noted in Section 3.1. The images from the VJ Technologies IXS High Frequency Integrated X-Ray Generator and the radiography camera were not expected to be identical since small positioning differences between the source, detector, and pipe as well as exposure time could cause differences in image intensity for the anomalies. The following sections describe in detail the evaluation of the testing parameters.

3.4.1 Detection of Defects – Qualitative Results

Detection of a single defect was determined by viewing the resulting image(s) of the defect and assessing that the technology did capture the defect in the appointed area. The defect location, size, and shape were known from previous mapping of the pipe. The presence of insulation was noted. The ability of the VJ Technologies IXS High Frequency Integrated X-Ray Generator to capture a defect was compared with findings from corresponding radiography camera image.

The weld images for Pipe Sample 1 were compared qualitatively. The weld region was divided into 10 areas or zones, enabling isolation of weld anomalies such as lack of penetration in the root pass, undercut in the crown, slag inclusion, porosity, as well as regions of acceptable welds. These welds were not high quality; rather, they were fabricated to hold the pipe together. Therefore, weld defects were expected with the potential for the entire weld to be defective. Figure 3-2 shows example placement of zones 1-5, with the remaining zones of similar dimension continuing below Zone 5. The presence or absence of defects in each zone was noted by the technology operator and then reported. Both weld images (0 º and 90 º images) were assessed. The zones were assessed in the circumferential direction in both images. The number and type of weld defects found by the VJ Technologies IXS High Frequency Integrated X-Ray Generator were compared qualitatively to the number and type of weld defects found by the radiography camera.

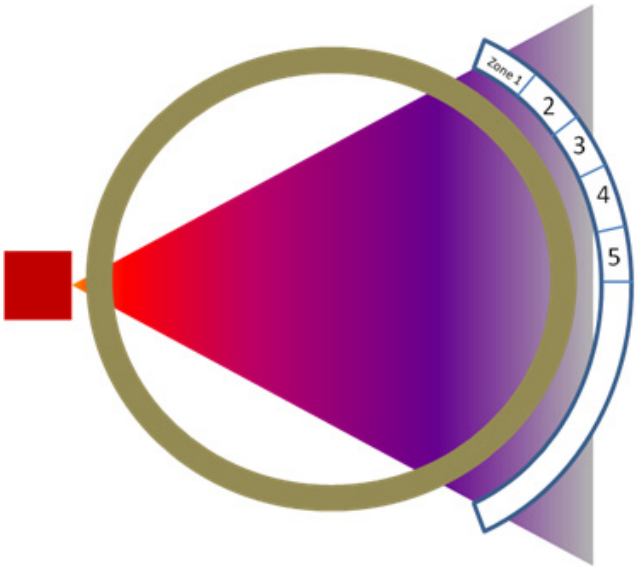

Figure 3-2. Assessment zones in the circumferential direction for Pipe Sample 1 weld with five zones shown as examples.

The performance of the VJ Technologies IXS High Frequency Integrated X-Ray Generator in detecting the natural corrosion on Pipe Sample 1 was evaluated by a similar process, dividing the natural corrosion region into 10 zones. The level of corrosion was noted by the technology operator with the qualitative terms of none, light, moderate, or heavy for defects in each zone. Both corrosion images were assessed and compared to actual corrosion depth measurements that had already been made in a previous mapping of the pipe. The corrosion levels found by the VJ Technologies IXS High Frequency Integrated X-Ray Generator were compared qualitatively to the levels found by the radiography camera and the actual corrosion depth measurements (see below for evaluation criteria).

- None: < 10% wall loss
- Light: 10% < depth < 25% wall loss
- Moderate: 25% < depth < 50% wall loss
- Heavy: > 50% wall loss

3.4.2 Detection of Defects – Quantitative Results

Quantitative measures were used to assess the performance of the VJ Technologies IXS High Frequency Integrated X-Ray Generator in measuring simulated corrosion anomalies on Pipe Sample 1. The images obtained by the x-ray and radiography camera were used to assess the following six parameters:

1. Axial extent (length) in inches
2. Circumferential extent (width) inches

3. Number of pits (typically 2 or 3)
4. Axial extent of deepest pit (pit length) in inches
5. Circumferential extent of deepest pit (pit width) inches
6. Depth of deepest pit (inches)

For the simulated defects (drilled holes) in Pipe Sample 2, the depth and diameter of each defect were assessed on each image collected by the VJ Technologies IXS High Frequency Integrated X-Ray Generator and the radiography camera.

3.4.3 Operational Factors

Operational factors to assess the sustainability of the technology include parameters such as maintenance needs, power needs, calibration frequency, data output, consumables used, ease of use, repair requirements, training and certification requirements, safety requirements and image throughput were evaluated based on testing observations and input provided from the vendor. Input was provided by the vendor, and Battelle technical staff also observed and recorded their own observations of these operational factors. Examples of information recorded included the daily status of diagnostic indicators for the technology, use or replacement of any consumables, use and nature of power supply needed to operate the technology, the effort or cost associated with maintenance or repair, vendor effort (e.g., time on site) for repair or maintenance, the duration and causes of any technology downtime or data acquisition failure, observations about technology startup, ease of use, clarity of the instruction manual, user-friendliness of any needed software, overall convenience of the technologies, the safety hazard associated with the use of the technology, and the number of images that could be collected and processed per hour or per day. These observations were summarized to aid in describing the technology performance in this verification report.

Chapter 4
Quality Assurance/Quality Control

QA/Quality Control (QC) procedures were performed in accordance with the quality management plan (QMP) for the AMS Center[5] and the test/QA plan for this verification test.[4]

4.1 Radiography Camera Reference Method and Vendor Technology QC

This verification test included a comparison of the VJ Technologies IXS High Frequency Integrated X-Ray Generator results to those of the radiography camera reference method. The quality of the reference measurements were assured by adherence to the requirements of the reference method, including the use of all applicable image quality indicators (IQIs). A one inch comparator ball wrapped in lead was used in every image collected by the radiography camera. The comparator ball is used to calibrate interpretation software to ensure exact line measurements and to confirm radiographic technique. This reference comparator (ball) indicated the sharpness of the image by providing a known actual dimension and a measured value on the image from which the sharpness could be calculated. The comparator ball was always clearly visible in all acceptable unprocessed images.

For the contact image, an ASTM B wire pack was used. The pack was two sheets of clear plastic that contained six wires arranged by increasing diameter. The diameter of the thinnest wire clearly visible on the image was used as a measure of IQI sensitivity. Four wires were visible on the contact image for the radiography camera. ASME 1025 stainless steel number 15 and 17 plaque hole penetrameters were also used on the contact image. A 2T sensitivity was obtained for each penetrameter using the radiography camera. No quality criteria were established for the contact images as these were not intended for measurement purposes but were used to determine differences in image quality between the tested devices. The data quality indicators as specified in the test/QA plan were met.

The same comparator ball as used by the radiography camera was also used in each image collected by the VJ Technologies IXS High Frequency Integrated X-Ray Generator. The comparator ball was always clearly visible in all acceptable images. The same ASTM B wire pack was also used for the contact image collected with the VJ Technologies IXS High Frequency Integrated X-Ray Generator. Five wires were visible on the resulting image. ASME 1025 stainless steel number 12, 15 and 17 plaque hole penetrameters were also used on the contact image. A 2T sensitivity was obtained for each penetrameter using the VJ Technologies IXS High Frequency Integrated X-Ray Generator.

4.2 Instrument/Equipment Testing, Inspection, Maintenance, and Calibration

The radiography camera does not require calibration. It is simply a shielding container for an isotope to be positioned from or retracted to. The source itself, however, does decay over time. A QSA Global Selenium-75 spherical source was used for the radiography camera. The original source activity was 89 Curies in January 2010. It had decayed to 41 Curies at the time of testing.

Manufacturer recommendations for calibration of the micrometer and calipers are related to usage patterns. The calipers and micrometer used in this test are not regularly used. Both instruments were inspected to observe that they attained zero measurement properly prior to be used in this verification test. Calibration was not performed prior to being used in this verification test. Calibration was not performed prior to the verification test in accordance with the manufacturer's guidance given the limited use history. As well, the level of accuracy needed from the calipers and micrometer for this test are approximately an order of magnitude higher than the actual accuracy of the instruments. As such, the lack of a recent calibration for the calipers and micrometer is not believed to impact their performance for this test.

The VJ Technologies IXS High Frequency Integrated X-Ray Generator was calibrated by the manufacturer according to the technology's specified procedures. This calibration was performed at the factory during the production of the specific VJ Technologies IXS High Frequency Integrated X-Ray Generator used for testing. The VJ Technologies IXS High Frequency Integrated X-Ray Generator comes factory-calibrated to the end user and does not otherwise require calibration. Techniques can be applied (such as the use of comparators and other image quality indicators) to determine image quality and assist in image interpretation.

4.3 Audits

Two types of audits were performed during the verification test: a technical systems audit (TSA) of the verification test performance and a data quality audit. Because of the nature of the samples evaluated in this verification test (i.e., defects on a pipe), a performance evaluation (PE) audit was not conducted as PE audit samples were not available. Audit procedures are described further below.

4.3.1 Technical Systems Audit

The Battelle Quality Assurance Officer (QAO) performed a TSA during this verification test. The purpose of this audit was to ensure that the verification test was being performed in accordance with the AMS Center QMP,[5] the test/QA plan,[4] and any standard operating procedures (SOPs) used by Battelle. In the TSA, the Battelle QAO reviewed the reference method used, compared actual test procedures to those specified or referenced in this plan, and reviewed data acquisition and handling procedures. The Battelle QAO also toured the test site, observed and reviewed the test procedures, and reviewed record books. He also checked calibration certifications for test measurement devices.

The TSA resulted in two observations, noting that one extra defect and a contact image, in addition to the defects called for in the test/QA plan, were imaged by both the radiography

camera and the vendor technology during testing. These observations did not detract from the quality of the data but served to augment it. A TSA report was prepared, and a copy was distributed to the EPA.

The EPA AMS Center Quality Manager also conducted an independent on-site TSA during the verification test. The TSA observations were communicated to technical staff at the time of the audit and afterward in a teleconference. No applicable findings were reported in either TSA.

4.3.2 Data Quality Audit

At least 25% of the data acquired during the verification test were audited. The Battelle QAO traced the data from the initial acquisition, through reduction and statistical comparisons, to final reporting to ensure the integrity of the reported results. All calculations performed on the data undergoing the audit were checked. The data quality audit resulted in two findings and two observations. The findings and observations were related to data tracking and labeling errors. All issues were resolved.

For one defect, P1-23, the assessment to measure pit length and width as performed by Mistras on the VJ Technologies IXS High Frequency Integrated X-Ray Generator image was not provided by Mistras for review as the image had been lost. As such, the measurement results for this defect could not be fully reviewed.

4.4 QA/QC Reporting

Each assessment and audit was documented in accordance with Sections 3.3.4 and 3.3.5 of the AMS Center QMP.[2] Once the audit reports were prepared, the Battelle Verification Test Coordinator ensured that a response was provided for each adverse finding or potential problem and implemented any necessary follow-up corrective action. The Battelle QA Manager ensured that follow-up corrective action was taken. The results of the TSA and data quality audit were submitted to the EPA.

4.5 Data Review

Records generated in the verification test received an independent internal review before these records were used to calculate, evaluate, or report verification results. Data were reviewed by a Battelle technical staff member involved in the verification test, but not the staff member who originally generated the data. The person performing the review added his or her initials and the date to a hard copy of the record being reviewed.

Chapter 5
Statistical Methods

The statistical methods and calculations used to evaluate the quantitative performance parameters listed in Section 3.1 are presented in this chapter.

5.1 Percent Error

The quantitative results were assessed by calculating the percent error between the actual and measured defect characteristics. For depth measurements, the pipeline industry typically normalizes the error to the wall thickness of the pipe rather than the actual reading.[6] This method is useful since small defects are not as important, but small errors on small defects can lead to large and misleading errors in percentages when actual depths are used as the normalizing factor. Percent error for depth measurements was calculated using the following equation:

$$\%Error = \frac{|Estimate - Actual|}{Wall\ Thickness} \times 100 \quad (1)$$

For all other measurements, percent error was calculated by dividing by the actual measurement.

5.2 Percent Difference

The quantitative results were also assessed by calculating the percent difference between the measurements made by the VJ Technologies IXS High Frequency Integrated X-Ray Generator and the radiography camera. This evaluation, in conjunction with the qualitative parameters, helped in assessing the performance of the VJ Technologies IXS High Frequency Integrated X-Ray Generator in relation to that of the reference technology results. Percent difference was calculated using the following:

$$\%Difference = \frac{(X\text{ - }Ray\ Technology\ Result - Radiography\ Camera\ Result)}{Radiography\ Camera\ Result} \times 100 \quad (2)$$

5.3 Operational Factors

Operational factors were determined based on documented observations of the testing staff. Operational factors are described qualitatively, not quantitatively; therefore, no statistical approaches were applied to the operational factors.

Chapter 6
Test Results

The results of the verification test of the VJ Technologies IXS High Frequency Integrated X-Ray Generator are presented below for each of the performance parameters. Note that only the VJ Technologies IXS High Frequency Integrated X-Ray Generator images and results that occurred during the re-testing on July 8, 2010 using the VMI 5100 system, software, and GE phosphor imaging plates are presented and evaluated in this section. Images from the VJ Technologies IXS High Frequency Integrated X-Ray Generator were collected by the vendor and processed by Mistras staff. The processed images were assessed by both Mistras (the same staff that evaluated the radiography camera image) and VJ Technologies. Defect evaluations were made using the StarrView 7 software using a 6 Megapixel monitor. Additionally, VJ Technologies evaluated the images using their VI-3 imaging software. The VI-3 software incorporated their Advanced Defect Enhancement (ADE) technology proprietary software to improve the visibility of the defects. The vendor then used the comparator ball measurements made by Mistras to calibrate the measurements in their software and took their own measurements of the defects. Reference images from the radiography camera were collected and assessed by Mistras staff. Mistras used the same StarrView 7 software package and 6 Megapixel monitor to evaluate the radiography camera images. Results from the evaluation of the IXS High Frequency Integrated X-Ray Generator images by both the vendor and Mistras are discussed in this section.

6.1 Detection of Defects – Qualitative Results

Both the radiography camera and the VJ Technologies IXS High Frequency Integrated X-Ray Generator were able to show the defect patches, natural corrosion, and weld under the insulation, as well as the defects on uninsulated pipe. Raw images were comparable in quality for non-contact images, as shown in Figure 6-1. After applying VJ Technologies ADE software to refine images, the x-ray technology images were clearer than those without adjustment. Figure 6-2 provides an example.

For defect P1-23, there were three pits in the defect. The radiography camera identified two pits, while the VJ Technologies IXS High Frequency Integrated X-Ray Generator identified all three pits. Depth measurements could only be determined for one defect using the x-ray device (P1-7) and two defects using the radiography camera (P1-7 and P1-11). These depth measurements were made based on the apparent depth of the patch and associated pits from the profile image. Depth measurements were not determined using the interior pipe wall, as would normally be done. Both the radiography camera and the x-ray device had difficulties detecting the interior pipe wall on the images. This led to an inability to make depth measurements on the defects. It

was suggested that the inability to detect the interior pipe wall could be related to the diameter of the pipes. The pipes used were larger in diameter than those typically imaged using the radiography and x-ray cameras.

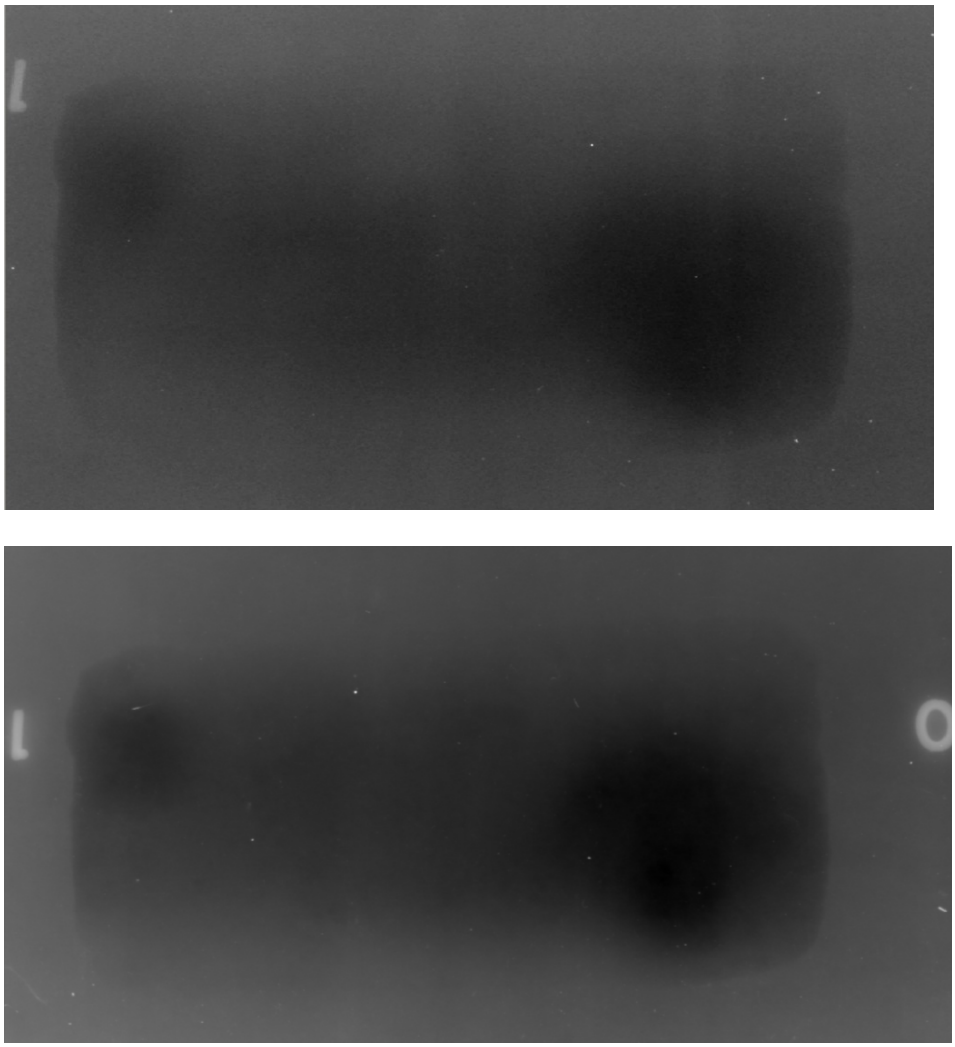

Figure 6-1. A comparison of radiography camera (top) and VJ Technologies IXS High Frequency Integrated X-Ray Generator (bottom) images with identical image processing applied.

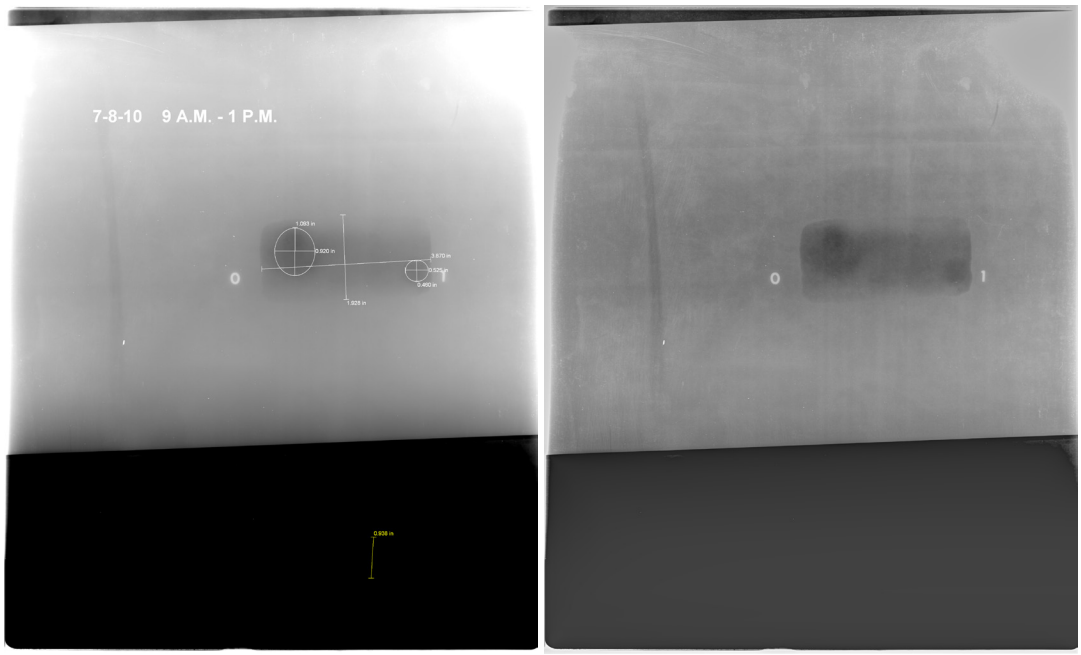

Figure 6-2. Example VJ Technologies IXS High Frequency Integrated X-Ray Generator results without adjustment (left) and with ADE adjustment (right).

For the contact images on Pipe Sample 2, the VJ Technologies IXS High Frequency Integrated X-Ray Generator provided a clearer image of the defects (see Figure 6-3). This is evidenced by the fact that more wires from the ASTM B wire pack were visible on the x-ray image (5 wires visible) than the radiography camera image (4 wires visible). The three simulated defects were well-defined in the x-ray image and the 2T holes in the penetrameter were readily visible.

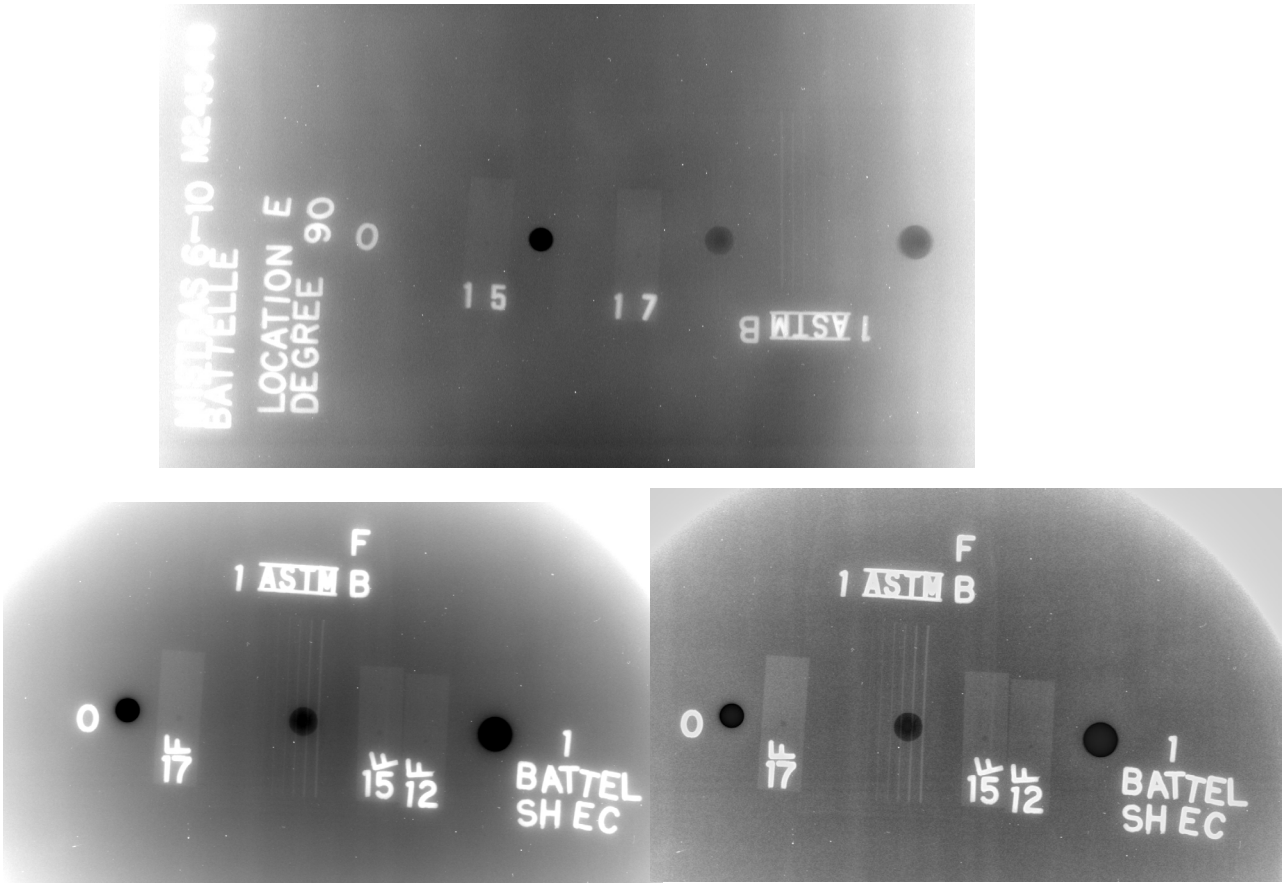

Figure 6-3. Pipe Sample 2 contact images for radiography camera (top) and VJ Technologies IXS High Frequency Integrated X-Ray Generator without adjustment (bottom left) and with ADE adjustment (bottom right).

For interpretation, the images containing the weld and the natural corrosion area from Pipe Sample 1 were used to assess the weld integrity. When assessing the weld, the image was divided into 10 equal zones (see Figure 3-2 for example zone placement) by the evaluator. Within each zone the weld was evaluated for root, crown, slag, and porosity defects. The weld was under insulation. Results for the radiography camera and the VJ Technologies IXS High Frequency Integrated X-Ray Generator are presented in Tables 6-1 through 6-3. Results in the tables are presented for the 90 º view, with difference in the 0 ° view noted. Based on previous characterization, the actual weld defects were noted to be incomplete penetration (IP) in all 10 zones. No other defects were determined.

Both devices noted IP in most of the 10 zones. Both the radiography camera and the x-ray device images, as interpreted by Mistras, indicated that there was one inch of acceptable weld in Zone 5. The Mistras representative was not able to determine weld defects in Zones 1 and 10 for the VJ Technologies IXS High Frequency Integrated X-Ray Generator images, while the VJ Technologies representative was able to determine IP in these zones using their proprietary software. Neither the radiography camera, nor the x-ray device found crown or slag defects on the weld, which is in agreement with the actual weld anomalies. The radiography camera image

indicated porosity in Zones 2, 3, 5, and 7. Porosity was noted in Zones 5, 6, and 7 in the interpretations of the VJ Technologies IXS High Frequency Integrated X-Ray Generator images.

Table 6-1. Weld Image Assessment Based on Radiography Camera Image

Zone	Root	Crown	Slag	Porosity	No Defect
1	IP	NA	NA	NA	NA
2	IP	NA	NA	Porosity[a]	NA
3	IP	NA	NA	NA[b]	NA
4	IP	NA	NA	NA	NA
5	Approximately 1 inch of OK weld[a]	NA	NA	Porosity[a]	NA
6	IP	NA	NA	NA	NA
7	IP	NA	NA	NA[b]	NA
8	IP	NA	NA	NA	NA
9	IP	NA	NA	NA	NA
10	IP	NA	NA	NA	NA

[a] Not noted in 0 ° view
[b] Porosity found in 0 ° view
NA – Not applicable (weld defect not observed)

Table 6-2. Weld Image Assessment by Mistras Based on VJ Technologies X-ray Image

Zone	Root	Crown	Slag	Porosity	No Defect
1	unable to determine	NA	NA	NA	NA
2	IP	NA	NA	NA	NA
3	IP	NA	NA	NA	NA
4	IP	NA	NA	NA	NA
5	IP[a]	NA	NA	NA[b]	NA
6	IP	NA	NA	Porosity[c]	NA
7	IP	NA	NA	NA	NA
8	IP	NA	NA	NA	NA
9	IP	NA	NA	NA	NA
10	unable to determine	NA	NA	NA	NA

[a] One inch of penetration noted in 0 ° view
[b] Porosity found in 0 ° view
[c] Not noted in 0 ° view
NA – Not applicable (weld defect not observed)

Table 6-3. Weld Image Assessment by VJ Technologies Based on VJ Technologies X-ray Image

Zone	Root	Crown	Slag	Porosity	No Defect
1	IP/Undercut[a]	NA	NA	NA	NA
2	IP/Undercut	NA	NA	NA	NA
3	IP/Undercut	NA	NA	NA	NA
4	IP/Undercut	NA	NA	NA	NA
5	IP/Undercut	NA	NA	NA	NA
6	IP/Undercut	NA	NA	NA	NA
7	IP/Undercut	NA	NA	Porosity	NA
8	IP/Undercut	NA	NA	NA	NA
9	IP/Undercut	NA	NA	NA	NA
10	IP/Undercut	NA	NA	NA	NA

[a] Difficult to separate IP from undercut on source side as weld suffers from both conditions
NA – Not applicable (weld defect not observed)

Both the radiography camera and the VJ Technologies IXS High Frequency Integrated X-Ray Generator were able to detect the natural corrosion area under the insulation on Pipe Sample 1. Pictures and details on the defect as determined in a previous characterization study prior to this verification test can be found in Appendix A. Tables 6-4 and 6-5 present the qualitative assessment of the natural corrosion area based on images from the radiography camera and the VJ Technologies IXS High Frequency Integrated X-Ray Generator using both the 90 ° view (Table 6-4) and the 0 ° view (Table 6-5). VJ Technologies did not provide interpretations of the natural corrosion area for the 0 ° view. The interpretations were based on contrast that was apparent in the image, not actual measurements. As with the qualitative assessment of the weld, the natural corrosion area was separated into 10 equal zones for its evaluation. Actual corrosion level assessments based on the previous characterization of Pipe Sample 1 are provided in each table. As noted in Section 3.4.1, the level of corrosion in the natural corrosion area was assessed based on the following guidelines:

- None: < 10% wall loss
- Light: 10% < depth < 25% wall loss
- Moderate: 25% < depth < 50% wall loss
- Heavy: > 50% wall loss

Results of the 90 ° view from the radiography camera are shown in Table 6-4. They were consistent with the actual corrosion levels in six of the 10 zones. The interpretations from the x-ray images agreed with the actual corrosion level in two and six of the 10 zones, depending on which software was used to perform the interpretations. The x-ray results agreed with the radiography camera results in six (Mistras evaluation) and four (VJ Technologies evaluation) of the zones.

For the 0 ° view results shown in Table 6-5, the radiography camera images were consistent with actual corrosion levels in five of the 10 zones. The results from the VJ Technologies IXS High Frequency Integrated X-Ray Generator agreed with the actual corrosion level estimates in four

zones. The radiography camera and VJ Technologies IXS High Frequency Integrated X-Ray Generator image interpretations were in agreement in two zones. Both of these interpretations were performed by the same Mistras representative.

Table 6-4. Assessment of Level of Corrosion for Natural Corrosion Area Using 90 º View Images from Radiography Camera (Radiography) and VJ Technologies IXS High Frequency Integrated X-Ray Generator (X-ray)

Zone	Actual	Radiography	X-ray (Mistras)	X-ray (VJ Technologies)
1	Moderate	Moderate	None	Light
2	Moderate	Moderate	Light	Light
3	Moderate	Moderate	Light	Heavy
4	Moderate	Moderate	Moderate	Moderate
5	Heavy	Moderate	Moderate	Moderate
6	Heavy	Moderate	Moderate	Heavy
7	Moderate	Moderate	Moderate	Moderate
8	Heavy	Moderate	Moderate	Heavy
9	Moderate	Light	Light	Moderate
10	Light	Light	None	Light

Table 6-5. Assessment of Level of Corrosion for Natural Corrosion Area Using 0 ° View Images from Radiography Camera (Radiography) and VJ Technologies IXS High Frequency Integrated X-Ray Generator (X-ray)

Zone	Actual	Radiography	X-ray (Mistras)
1	Light	Moderate	None
2	Light	Moderate/Heavy	None
3	Moderate	Moderate	Light
4	Moderate	Heavy	Moderate
5	Heavy	Moderate/Heavy	Heavy
6	Moderate	Moderate	Moderate
7	Moderate	Moderate	Light
8	Light	Heavy	Light
9	Light	Moderate	None
10	Light	Light	None

6.2 Detection of Defects – Quantitative Results

Quantitative measurements were made for defects P1-1, P1-18, and P1-23 on Pipe Sample 1 as well as the simulated defects on Pipe Sample 2. Each defect area on Pipe Sample 1 had two or three pits. There were three simulated defects on Pipe Sample 2. Using the comparator ball to calibrate the measurements, the images of each defect from the radiography camera and VJ

Technologies IXS High Frequency Integrated X-Ray Generator were measured using software to determine the length, width, and depth of each pit as well as the overall length and width of the defect patch. Appendix A provides pictures and details from a previous characterization study prior to this verification test for the defects on Pipe Sample 1. A picture of the Pipe Sample 2 simulated defects is provided in Figure 6-4. Results for the quantitative measurements are discussed in the following sections.

Figure 6-4. Uninsulated Pipe Sample 2 simulated defects.

6.2.1 Percent Error

Percent error measurements were calculated for both the radiography camera and VJ Technologies IXS High Frequency Integrated X-Ray Generator images for each of the defect measurements reported. As discussed in Section 5.1, the percent error calculations were normalized to the wall thickness of the pipe being imaged for pit depth. For Pipe Sample 1, the wall thickness was 0.188 inches. This thickness measurement was used for determining percent error on defects P1-1, -7, -18, and -23. P1-7, -18, and -23 were under insulation; P1-1 was not. The Pipe Sample 2 wall thickness was 0.515 inches. The individual pits in each defect were contained in an overall patch of corrosion that was rectangular in shape. The length and width of each patch was evaluated by each device, along with the measurements of the individual pits within the patch.

Percent errors for the measurements on defect P1-7 are presented in Table 6-6. Actual measurements as well as measurements from the radiography camera and VJ Technologies IXS High Frequency Integrated X-Ray Generator images are also presented. Percent errors ranged from 5 to 46% for the radiography camera results. The lowest errors (5 and 6%) were found for the patch length and width measurements while the highest errors were found in measuring the length, width, and depth of the pits in the defect. Percent error for the VJ Technologies IXS High Frequency Integrated X-Ray Generator image measurements ranged from 0 to 51%. Percent errors were higher in the Mistras interpretation of the defect using the VMI StarrView 7 software. Defect measurements made by VJ Technologies using their ADE software had a

smaller range of errors, from 14 to 31%. Percent errors in determining the pit lengths and widths from the VJ Technologies IXS High Frequency Integrated X-Ray Generator images were similar to the radiography camera image measurements using the same software. Pit depths could not be determined from the x-ray images. However, patch depth was determined from the by VJ Technologies' analysis of the images. This was included as a surrogate measure of pit depth in Table 6-6. Both the radiography camera and the x-ray device were able to find both pits in the defect patch.

Table 6-6. Defect P1-7 Measurements (in Inches) and Percent Error Results

	Actual	Radiography	% Error	X-ray (Mistras)	% Error	X-ray (VJ Technologies)	% Error
Patch Length (in)	2.0	1.9	5	2.0	0	2.1	2
Patch Width (in)	1.9	1.8	6	1.8	4	1.9	2
Number of Pits	2.0	2.0	-	2.0	-	2.0	-
Pit1 Length (in)	0.60	0.41	32	0.42	30	0.52	14
Pit 2 Length (in)	0.60	0.39	35	0.30	51	0.48	19
Pit 1 Width (in)	0.60	0.36	40	0.39	35	0.55	8
Pit 2 Width (in)	0.50	0.27	46	0.26	48	0.42	17
Pit 1 Depth (in)	0.14	0.08	33	UTD	NA	0.08	31
Pit 2 Depth (in)	0.13	0.09	20	UTD	NA	0.08	26

UTD – Unable to determine
NA – Not applicable. Pit depth measurements were not able to be determined.

Percent errors for the measurements on defect P1-18 are presented in Table 6-7. Ranges of percent errors for measurements made from the radiography camera and VJ Technologies IXS High Frequency Integrated X-Ray Generator images were similar to those determined for defect P1-7. Percent errors for defect P1-18 ranged from 7 to 31% for the radiography camera and 3 to 56% for the VJ Technologies IXS High Frequency Integrated X-Ray Generator. Pit depth measurements could not be made from any of the images. For the radiography camera, errors in the measurements of Pit 1 and Pit 2 were similar and higher than errors in the measurement of the patch dimensions. Reduced error was found in the measurement of Pit 2 length and width using the VJ Technologies IXS High Frequency Integrated X-Ray Generator images as compared to the radiography camera results. Measurements made on the Pit 1 length and width by VJ Technologies resulted in increased error over the same measurements made by Mistras on the x-ray images as well as those made using the radiography camera images. Measurements of patch length and width as determined using the VJ Technologies IXS High Frequency Integrated X-Ray Generator images had errors slightly lower for length and higher for width as compared to the radiography camera results.

Table 6-8 provides the percent errors and measurements for defect P1-23. This defect had three pits. Two were detected by the radiography camera. The x-ray device identified all three pits. The percent errors for measurement of the patch length and width using the radiography camera image were 37% for both. Percent errors for these measurements were 4.6 to 37 times lower for

the images made by the VJ Technologies IXS High Frequency Integrated X-Ray Generator. Percent errors for the measurement of pit length and width varied for both devices. Pit 3 measurements had the lowest percent error based on images from the VJ Technologies IXS High Frequency Integrated X-Ray Generator determined by Mistras using the VMI StarrView 7 software. Pit depth measurements could not be determined from the VJ Technologies IXS High Frequency Integrated X-Ray Generator images.

Table 6-7. Defect P1-18 Measurements (in Inches) and Percent Error Results

	Actual	Radiography	% Error	X-ray (Mistras)	% Error	X-ray (VJ Technologies)	% Error
Patch Length (in)	4.0	3.7	7	3.9	3	4.1	3
Patch Width (in)	1.7	1.8	8	1.9	13	2.0	18
Number of Pits	2.0	2.0	-	2.0	-	2.0	-
Pit 1 Length (in)	1.4	1.0	28	0.92	34	0.69	51
Pit 2 Length (in)	0.50	0.40	20	0.52	5	0.52	3
Pit 1 Width (in)	1.3	0.90	31	1.1	16	0.57	56
Pit 2 Width (in)	0.50	0.36	28	0.46	8	0.62	24
Pit 1 Depth (in)	0.15	UTD	NA	UTD	NA	UTD	NA
Pit 2 Depth (in)	0.12	UTD	NA	UTD	NA	UTD	NA

UTD – Unable to determine
NA – Not applicable. Pit depth measurements were not able to be determined.

Table 6-8. Defect P1-23 Measurements (in Inches) and Percent Error Results

	Actual	Radiography	% Error	X-ray (Mistras)	% Error	X-ray (VJ Technologies)	% Error
Patch Length (in)	3.7	2.3	37	3.8	4	3.8	1
Patch Width (in)	1.7	1.1	37	1.6	8	1.8	5
Number of Pits	3.0	2.0	-	3.0	-	3.0	-
Pit1 Length (in)	0.30	0.40	34	0.52	72	0.65	118
Pit 2 Length (in)	0.50	Not Seen	NA	0.75	50	0.96	93
Pit 3 Length (in)	0.80	0.49	39	0.75	7	1.0	30
Pit 1 Width (in)	0.20	0.32	60	0.47	136	0.52	159
Pit 2 Width (in)	0.60	Not Seen	NA	0.72	20	0.79	31
Pit 3 Width (in)	0.70	0.48	32	0.69	1	0.68	3
Pit 1 Depth (in)	0.05	0.04	4	UTD	NA	UTD	NA
Pit 2 Depth (in)	0.07	Not Seen	NA	UTD	NA	UTD	NA
Pit 3 Depth (in)	0.09	0.07	13	UTD	NA	UTD	NA

UTD – Unable to determine
NA – Not applicable. Pit depth measurements were not able to be determined.

Table 6-9 provides the percent errors and measurements for defect P1-1, the uninsulated defect on Pipe Sample 1. Both pits were detected in images from both the radiography camera as well as the VJ Technologies IXS High Frequency Integrated X-Ray Generator. Pit depths were not able to be determined on images from either device. Percent errors were the largest for both devices on the measurement of width for Pit 1. The percent errors for patch length and width measurements were similar between the two devices. The percent errors were lowest for the VJ Technologies ADE software interpretations.

Table 6-9. Defect P1-1 Measurements (in Inches) and Percent Error Results

	Actual	Radiography	% Error	X-ray (Mistras)	% Error	X-ray (VJ Technologies)	% Error
Patch Length (in)	2.0	1.9	6	1.9	5	2.0	2
Patch Width (in)	1.9	1.9	2	1.9	2	1.9	1
Number of Pits	2.0	2.0	-	2.0	-	2.0	-
Pit1 Length (in)	0.50	0.34	32	0.37	26	0.45	11
Pit 2 Length (in)	0.50	0.52	5	0.60	20	0.50	1
Pit 1 Width (in)	0.70	0.30	57	0.32	54	0.50	29
Pit 2 Width (in)	0.40	0.50	24	0.58	45	0.38	6
Pit 1 Depth (in)	0.15	UTD	NA	UTD	NA	UTD	NA
Pit 2 Depth (in)	0.13	UTD	NA	UTD	NA	UTD	NA

UTD – Unable to determine
NA – Not applicable. Pit depth measurements were not able to be determined.

Table 6-10 presents measurements and percent errors for the simulated defects on the uninsulated Pipe Sample 2. Percent errors for all measurements for both the radiography camera and the VJ Technologies IXS High Frequency Integrated X-Ray Generator were $\leq 5\%$ in all cases but one. These are the most consistently low percent errors seen for any defects. As evidenced in the images, the definition of the simulated defects was more pronounced than with the other defects, including the uninsulated defect on Pipe Sample 1. This is likely related to the fact that these were clearly defined holes in the pipe and not a patch of corrosion with pits in it. Pit depth could not be determined from any image for either device.

Table 6-10. Measurements (in Inches) and Percent Error Results for Drilled Defects on Pipe Sample 2

	Actual	Radiography	% Error	X-ray (Mistras)	% Error	X-ray (VJ Technologies)	% Error
Pit 1 Diameter (in)	0.38	0.36	4	0.39	3	0.34	9
Pit 1 Depth (in)	0.19	UTD	NA	UTD	NA	UTD	NA
Pit 2 Diameter (in)	0.31	0.32	1	0.33	4	0.30	4
Pit 2 Depth (in)	0.12	UTD	NA	UTD	NA	UTD	NA
Pit 3 Diameter (in)	0.25	0.25	3	0.26	5	0.25	2
Pit 3 Depth (in)	0.32	UTD	NA	UTD	NA	UTD	NA

UTD – Unable to determine
NA – Not applicable. Pit depth measurements were not able to be determined.

Tables 6-6 through 6-10 present percent error measurements for each individual defect and the measurements associated with each defect. For each defect, measurements were made for different characteristics of the defect (i.e., patch length, patch width, pit length, etc.). Each of these characteristics was evaluated for each defect. In an effort to provide a better overall understanding of how the VJ Technologies IXS High Frequency Integrated X-Ray Generator performed in comparison to actual measurements, average percent errors were calculated for each defect characteristic across all defects. For example, the percent errors for patch length for defect P1-7, -18, -23, and -1, were averaged and the pit length errors for all of the pits in defect P1-7, -18, -23, and -1 and Pipe Sample 2 were averaged. These average percent errors, along with their associated standard deviation, are presented in Table 6-11.

Table 6-11. Average Percent Error and Standard Deviation (StDev) Results for All Percent Errors Reported in Tables 6-6 Through 6-10 for Individual Defect Measurement Categories

	Radiography	StDev	X-ray (Mistras)	StDev	X-ray (VJT)	StDev
Patch Length	14	15	3	2	2	1
Patch Width	13	16	7	5	6	8
Pit Length	28	11	33	22	38	42
Pit Width	30	21	31	38	29	44
Pit Depth	18	12	NA	NA	29	4

NA – Not applicable. Pit depth measurements were not able to be determined.

Average percent errors for the radiography camera ranged from 13% for all patch width measurements to more than twice that with 28 and 30% errors for all pit length and width measurements, respectively. Standard deviations for the radiography camera average errors were

similar across the different measurement categories (i.e., patch length and width and pit length, width, and depth). The average percent error range was wider for the results for the VJ Technologies IXS High Frequency Integrated X-Ray Generator, ranging from 2 to 38% average error. Measurement of all pit lengths and depths from the VJ Technologies IXS High Frequency Integrated X-Ray Generator images as determined using the VMI StarrView 7 software and the VJ Technologies ADE software were similar across all defects and similar to the average percent errors for the radiography camera, indicating that measurements were able to be obtained from images from both devices with similar accuracy. The average percent error for all patch lengths and widths based on images from the VJ Technologies IXS High Frequency Integrated X-Ray Generator was two to seven times lower than those for the radiography camera. The standard deviations for these average errors were also smaller for the vendor's device, indicating that patch dimensions were more accurately determined using the VJ Technologies IXS High Frequency Integrated X-Ray Generator images.

A variable sensitivity analysis of the method used to predict the remaining strength of corroded pipe, ASME Standard B31G, shows that this method is more sensitive to wall thickness than to length or width. The radiography camera was able to assess depth more often (four out of 12 pits) than the VJ Technologies IXS High Frequency Integrated X-Ray Generator (two out of 12 pits). When both were able measure depth, the radiography camera was 50% more accurate. However, the interior pipe walls were not defined in images from either technology, so depth measurements were not able to be made based on the internal pipe wall. However, depth measurements could be made by basing measurements on the exterior wall. The ASME assessment criteria are not as sensitive to errors in length estimations. Length errors that are on the order of a wall thickness or two are typically tolerable. For all length measurements made, the radiography camera had one significant error while the VJ Technologies IXS High Frequency Integrated X-Ray Generator did not have any. The radiography camera's error was with the shallowest of the four patches tested. Quantification of the edges of shallow corrosion is often difficult, but these anomalies usually do not affect structural performance. The width estimate is the least important parameter in corrosion characterization and is often omitted by the assessment methodologies.

6.2.2 Percent Difference

Percent difference was calculated for the VJ Technologies IXS High Frequency Integrated X-Ray Generator measurement results in comparison with the radiography camera results. Percent difference calculations were made for all measurements on each defect. Percent difference was also calculated for each set of interpretations on the x-ray images (i.e., those measurements made by Mistras and those by VJ Technologies and their ADE software). Percent differences were calculated for defects P1-7, P1-18, and P1-23 that were under insulation on Pipe Sample 1; defect P1-1 that was uninsulated on Pipe Sample 1; and the simulated defects on Pipe Sample 2 that were uninsulated.

Percent difference results for the defect P1-7 are provided in Table 6-12. Percent differences ranged from -24 to 56%. Within the Mistras interpretation method, the percent differences were low; with all but two measurements showing positive percent differences less than 10%. Positive percent differences indicate that the VJ Technologies IXS High Frequency Integrated X-

Ray Generator measurement estimates were larger than those made from the radiography camera images. When compared to the x-ray device interpretations by Mistras, measurements for Pit 2 were larger for the radiography camera image. Pit width and depth measurements were the largest based on interpretations by VJ Technologies.

Table 6-12. Defect P1-7 Measurements (in Inches) and Percent Difference Results

	Radiography	X-ray (Mistras)	% Difference	X-ray (VJ Technologies)	% Difference
Patch Length (in)	1.9	2.0	6	2.0	8
Patch Width (in)	1.8	1.8	2	1.9	4
Pit1 Length (in)	0.41	0.42	3	0.52	27
Pit 2 Length (in)	0.39	0.30	-24	0.48	24
Pit 1 Width (in)	0.36	0.39	8	0.55	53
Pit 2 Width (in)	0.27	0.26	-3	0.42	56
Pit 1 Depth (in)	0.08	UTD	NA	0.08	4
Pit 2 Depth (in)	0.09	UTD	NA	0.08	-13

UTD – Unable to determine
NA – Not applicable. Pit depth measurements were not able to be determined.

Defect P1-18 percent difference results are provided in Table 6-13. The difference between the patch length and width measurements for the two devices using the VMI StarrView 7 software was 4 and 5%, respectively. Differences in pit measurements, however, were higher, up to nine times for the Pit 2 width measurements. The percent difference for Pit 2 width as estimated by the VJ Technologies ADE software was even higher at 73%. Only Pit 1 measurements were larger for the radiography camera than the VJ Technologies IXS High Frequency Integrated X-Ray Generator.

Table 6-13. Defect P1-18 Measurements (in Inches) and Percent Difference Results

	Radiography	X-ray (Mistras)	% Difference	X-ray (VJ Technologies)	% Difference
Patch Length (in)	3.7	3.9	4	4.1	11
Patch Width (in)	1.8	1.9	5	2.0	10
Pit1 Length (in)	1.0	0.92	-9	0.69	-31
Pit 2 Length (in)	0.40	0.52	32	0.52	29
Pit 1 Width (in)	0.90	1.1	22	0.57	-36
Pit 2 Width (in)	0.36	0.46	28	0.62	73
Pit 1 Depth (in)	UTD	UTD	NA	UTD	NA
Pit 2 Depth (in)	UTD	UTD	NA	UTD	NA

UTD – Unable to determine
NA – Not applicable. Pit depth measurements were not able to be determined.

Percent differences between the radiography camera and VJ Technologies IXS High Frequency Integrated X-Ray Generator image measurements were generally higher for P1-23, as shown in Table 6-14, then those found for P1-18 (see Table 6-13). The measurements based on images from the x-ray technology were always higher than those based on the radiography camera, thus resulting in positive percent errors. Percent differences ranged from 28 to 65% with one measurement for Pit 3 using the VJ Technologies ADE software resulting in a 113% difference from the radiography camera result. Pit 2 was not seen in the radiography camera image but was measureable in the VJ Technologies IXS High Frequency Integrated X-Ray Generator image. However, comparisons to the radiography camera results could not be made.

Table 6-14. Defect P1-23 Measurements (in Inches) and Percent Difference Results

	Radiography	X-ray (Mistras)	% Difference	X-ray (VJ Technologies)	% Difference
Patch Length (in)	2.3	3.8	65	3.8	60
Patch Width (in)	1.1	1.6	44	1.8	65
Pit1 Length (in)	0.40	0.52	28	0.65	62
Pit 2 Length (in)	Not Seen	0.75	NA	0.96	NA
Pit 3 Length (in)	0.49	0.75	52	1.0	113
Pit 1 Width (in)	0.32	0.47	48	0.52	62
Pit 2 Width (in)	Not Seen	0.72	NA	0.79	NA
Pit 3 Width (in)	0.48	0.69	45	0.68	42
Pit 1 Depth (in)	0.04	UTD	NA	UTD	NA
Pit 2 Depth (in)	Not Seen	UTD	NA	UTD	NA
Pit 3 Depth (in)	0.07	UTD	NA	UTD	NA

UTD – Unable to determine
NA – Not applicable. Pit depth measurements were not able to be determined.

Percent differences were lower for the defect P1-1 measurements. As Table 6-15 shows, percent difference ranged from -24 to 31% with one measurement for Pit 1 width using the VJ Technologies ADE software resulting in a 64% difference from the radiography camera result. The measurement estimates reported by Mistras from the x-ray device images had a smaller overall range, with percent differences from -4 to 17%. Pit 2 measurements had the largest percent differences in this range at 14% for length and 17% for width measurements. Patch length and width measurements for the VJ Technologies IXS High Frequency Integrated X-Ray Generator image were within 4% of the radiography camera results. P1-1 was the uninsulated defect on Pipe Sample 1.

Table 6-15. Defect P1-1 Measurements (in Inches) and Percent Difference Results

	Radiography	X-ray (Mistras)	% Difference	X-ray (VJ Technologies)	% Difference
Patch Length (in)	1.9	1.9	1	2.0	4
Patch Width (in)	1.9	1.9	-4	1.9	-1
Pit1 Length (in)	0.34	0.37	9	0.45	31
Pit 2 Length (in)	0.52	0.60	14	0.50	-5
Pit 1 Width (in)	0.30	0.32	5	0.50	64
Pit 2 Width (in)	0.50	0.58	17	0.38	-24
Pit 1 Depth (in)	UTD	UTD	NA	UTD	NA
Pit 2 Depth (in)	UTD	UTD	NA	UTD	NA

UTD – Unable to determine
NA – Not applicable. Pit depth measurements were not able to be determined.

As with the percent error results, percent difference results for the simulated defects in Pipe Sample 2 (see Table 6-16) were among the lowest obtained for all defects. Low percent differences were obtained for all measurements, with percent differences ranging from -5 to 8%. Depth measurements could not be determined for any of the pits in this defect. Only measurements made using the VJ Technologies ADE software produced estimates that were smaller than the radiography camera image measurements.

Table 6-16. Measurements (in Inches) and Percent Difference Results for Drilled Defects on Pipe Sample 2

	Radiography	X-ray (Mistras)	% Difference	X-ray (VJ Technologies)	% Difference
Pit 1 Diameter (in)	0.36	0.39	7	0.34	-5
Pit 1 Depth (in)	UTD	UTD	NA	UTD	NA
Pit 2 Diameter (in)	0.32	0.33	3	0.30	-5
Pit 2 Depth (in)	UTD	UTD	NA	UTD	NA
Pit 3 Diameter (in)	0.25	0.26	8	0.25	1
Pit 3 Depth (in)	UTD	UTD	NA	UTD	NA

UTD – Unable to determine
NA – Not applicable. Pit depth measurements were not able to be determined.

Table 6-17. Average Percent Difference and Standard Deviation (StDev) Results for All Percent Differences Reported in Tables 6-12 through 6-16 for Individual Defect Measurement Categories

	X-ray (Mistras)	StDev	X-ray (VJT)	StDev
Patch Length	19	31	21	27
Patch Width	14	20	20	30
Pit Length	21	16	40	33
Pit Width	18	16	38	26
Pit Depth	NA	NA	8	6

As in Table 6-11, average percent differences were calculated for each defect characteristic across all defects. The absolute value of all individual percent differences was used in the average calculations. Thus, there is no indication of which measurement was greater (that from the radiography camera or that from the VJ Technologies IXS High Frequency Integrated X-Ray Generator) in the averages. Tables 6-12 through 6-16 show that estimate of defect characteristics made using the radiography camera were greater than those made using the VJ Technologies IXS High Frequency Integrated X-Ray Generator in four instances as determined by Mistras and in seven instances as determined using the VJ Technologies ADE software. In all other cases, the measurement estimates made using the VJ Technologies IXS High Frequency Integrated X-Ray Generator were greater than those made using the radiography camera images. The average percent differences, along with their associated standard deviation, are presented in Table 6-17.

Average percent differences for the VJ Technologies IXS High Frequency Integrated X-Ray Generator ranged from 14% for all patch width measurements to 40% for all pit length measurements. Standard deviations were similar for patch width and length measurements, regardless of who interpreted the images. Standard deviations for pit length and width measurements were greater for estimates made using the VJ Technologies ADE software.

One corrosion patch was not assessed as well as the other four. Individual percent differences for patch length and width for four of the defects ranged from -5 to 11%. This percent difference would typically have minimal effect on pipeline assessment calculations. The higher average percent difference for patch length and width are driven by large percent differences ranging from 44 to 65% for defect P1-23. Though these values indicate a large difference from the radiography camera results for these measurements, it should be noted that the VJ Technologies IXS High Frequency Integrated X-Ray Generator results were actually closer to the actual measured value for this defect (1 to 8% percent error for the VJ Technologies IXS High Frequency Integrated X-Ray Generator versus 37% error for the radiography camera). The patch with the high error was also the shallowest. In pipeline assessments, it is more important to assess length of corrosion patches when the depth is greater, which both techniques did in defects P1-7, -18, -1, and PS2.

Average percent differences between the VJ Technologies IXS High Frequency Integrated X-Ray Generator and radiography camera results were less than 22% for all defect measurement categories for interpretations made using the VMI StarrView 7 software. Larger percent differences of 40 and 38% for pit length and width (respectively) found from images interpreted using the VJ Technologies ADE software were driven mainly by large individual percent difference for defect P1-23 (see Table 6-14).

Table 6-17 shows that for most tests, the pit depth was not able to be visualized; but typically depth is the most important measurement in pipeline assessments. The average percent difference for pit depth measurements for the VJ Technologies ADE software was based on two individual pit depth measurements.

6.3 Operational Factors

The VJ Technologies IXS High Frequency Integrated X-Ray Generator required the use of a typical 110 V or 220 V power outlet to operate the technology. A connection to a computer was also required to program the x-ray device for taking images. The computer and associated software controlled the power output of the VJ Technologies IXS High Frequency Integrated X-Ray Generator and turned the tube on and off. The exposure time is determined by the user and is controlled by manually turning the device on and off. The exposure time was recorded by a simple stopwatch or timing device during testing.

The imaging exposure time used for this test was 1 minute. This time is adjustable to the needs of the project. In order to determine an appropriate exposure time and source power, initial images were collected and evaluated until the proper exposure situation was determined. This process took approximately one hour. Preparation of the VJ Technologies IXS High Frequency Integrated X-Ray Generator involved setting it up on a tripod stand and attaching the imaging plate and associated markers and image quality indicators to the pipe and inputting the correct parameters into the software. This process took approximately 10 to 15 minutes for each image. Similar preparation times were noted for the radiography camera. Positioning the VJ Technologies IXS High Frequency Integrated X-Ray Generator for images above the pipe required the use of a platform to suspend the device the proper distance above the pipe. The radiography camera did not require substantial equipment (i.e., a platform or any such device) to collect images above the pipe.

The x-ray device was placed 28 inches away from the defect (except for the contact image) and was operated at 3 mA and 160 kV. The radiography camera was 32 inches away from the pipe and used an exposure time of 1.5 minutes.

The VJ Technologies IXS High Frequency Integrated X-Ray Generator weighs approximately 59 pounds and is a self-contained unit with electrical and computer cables, as well as a computer, needed for operation. The x-ray tube in the unit has a life span of six to eight years. The radiography camera weighs approximately 50 pounds. A radioactive source, guide tube, and drive cable are needed for its operation. No computer or electricity is needed for the radiography camera. The 89 Curies Selenium 75 source will have decayed by a factor of eight down to 11 Curies in one year from its purchase, with a subsequent increase in necessary exposure times.

The VJ Technologies IXS High Frequency Integrated X-Ray Generator produces radiation, though not from a radioactive source. Thus, an operator must be properly licensed to handle radiation safely. This technology is also intended to be used by field staff experienced in performing pipeline inspections. To account for the emission of radiation from the VJ Technologies IXS High Frequency Integrated X-Ray Generator, a radiation safety boundary had to be established prior to the operation of the device. Figure 6-5 shows the radiation safety boundaries used for the VJ Technologies IXS High Frequency Integrated X-Ray Generator. These boundaries were similar to those established for the radiography camera.

No maintenance or calibration was needed for the VJ Technologies IXS High Frequency Integrated X-Ray Generator. The technology came calibrated from the factory and does not need further calibration at any point of its operation. The technology is rated to perform in temperatures up to 30 ºC. The day of testing, it was very hot and sunny, with temperatures reaching upwards of 32 ºC. Images were collected between 9 a.m. and 1 p.m. Similar conditions were encountered during the testing of the radiography camera. There were no operational issues during the verification testing.

Figure 6-5. Radiation safety boundary for the operation of the VJ Technologies IXS High Frequency Integrated X-Ray Generator.

Phosphor imaging plates were used to record the images collected by the VJ Technologies IXS High Frequency Integrated X-Ray Generator. Generally, these plates are continually reused when taking images. Significant ghosting was noted on the imaging plates when using this

technology. That is, images from previous images using the VJ Technologies IXS High Frequency Integrated X-Ray Generator were burned onto the plate and could not be cleared. These burned images did not appear to impact the ability of the VJ Technologies IXS High Frequency Integrated X-Ray Generator to take new images or interfere with the interpretation of any images, but they remained on the imaging plates and rendered them useless after the testing was completed. The cost of each phosphor imaging plate was approximately $500.

Testing was originally conducted using an AllPro scanner and GE Rhythm software for processing the VJ Technologies IXS High Frequency Integrated X-Ray Generator images. Proper images were not able to be obtained using these processing components. Retesting was conducted, and images from the VJ Technologies IXS High Frequency Integrated X-Ray Generator were processed using the VMI 5100 computed radiography scanner and associated StarrView 7 software. Image processing took less than 1 minute. No problems were encountered with this processing.

Chapter 7
Performance Summary

The VJ Technologies IXS High Frequency Integrated X-Ray Generator showed defect patches, natural corrosion, and weld under the insulation, as well as the defects on uninsulated pipe. Raw images were comparable in quality to the radiography camera images for non-contact images. For the contact image, the VJ Technologies IXS High Frequency Integrated X-Ray Generator provided a clearer image of the defects. For defect P1-23, there were three pits in the defect. The radiography camera identified two pits, while the VJ Technologies IXS High Frequency Integrated X-Ray Generator identified all three pits. Both the radiography camera and the x-ray device had difficulties detecting the interior pipe wall on the images. This often led to an inability to make depth measurements on the defects for both the radiography camera and the x-ray technology. Depth measurements were determined for one defect using the x-ray device (P1-7) and two using the radiography camera (P1-7 and P1-11).

Tables 7-1 and 7-2 provide measurement results for each of the defects evaluated in this verification test. Results are shown for estimates made from both the radiography camera and the VJ Technologies IXS High Frequency Integrated X-Ray Generator images. For the VJ Technologies IXS High Frequency Integrated X-Ray Generator images, interpretations were made by both the same Mistras staff who interpreted the radiography camera images (using the same VMI StarrView 7 software package) and by the vendor using their own ADE software application. Table 7-1 provides results from defects under insulation on Pipe Sample 1. Table 7-2 provides results from the uninsulated defect on Pipe Samples 1 and 2. Pit depth measurements could not be determined in all but one of the VJ Technologies IXS High Frequency Integrated X-Ray Generator images.

Average percent differences were calculated for each defect characteristic (e.g., pit length, patch width, etc.) across all defects and ranged from 14% for all patch width measurements to 40% for all pit length measurements. Standard deviations were similar for patch width and length measurements.

Average percent errors for the radiography camera ranged from 13% for all patch width measurements to more than twice that with 28 and 30% errors for all pit length and width measurements, respectively. Standard deviations for the radiography camera average errors were similar across the different measurement categories (i.e., path length, pit width, etc.). The average percent error range was wider for the results for the VJ Technologies IXS High Frequency Integrated X-Ray Generator, ranging from 2 to 38% average error.

Table 7-1. Summary of VJ Technologies IXS High Frequency Integrated X-Ray Generator Percent Error and Percent Difference (% Diff) Results for Defects under Insulation

Defect P1-7	Actual	Radiography	% Error	X-ray (Mistras)[a]	% Error	% Diff	X-ray (VJT)[b]	% Error	% Diff
Patch Length (in)	2.0	1.9	5	2.0	0	6	2.1	2	8
Patch Width (in)	1.9	1.8	6	1.8	4	2	1.9	2	4
Number of Pits	2.0	2.0		2.0			2.0		
Pit1 Length (in)	0.60	0.41	32	0.42	30	3	0.52	14	27
Pit 2 Length (in)	0.60	0.39	35	0.30	51	-24	0.48	19	24
Pit 1 Width (in)	0.60	0.36	40	0.39	35	8	0.55	8	53
Pit 2 Width (in)	0.50	0.27	46	0.26	48	-3	0.42	17	56
Pit 1 Depth (in)	0.14	0.08	33	UTD	NA	NA	0.08	31	4
Pit 2 Depth (in)	0.13	0.09	20	UTD	NA	NA	0.08	26	-13
Defect P1-18									
Patch Length (in)	4.0	3.7	7	3.9	3	4	4.1	3	11
Patch Width (in)	1.7	1.8	8	1.9	13	5	2.0	18	10
Number of Pits	2.0	2.0		2.0			2.0		
Pit1 Length (in)	1.4	1.0	28	0.92	34	-9	0.69	51	-31
Pit 2 Length (in)	0.50	0.40	20	0.52	5	32	0.52	3	29
Pit 1 Width (in)	1.3	0.89	31	1.1	16	22	0.57	56	-36
Pit 2 Width (in)	0.50	0.36	28	0.46	8	28	0.62	24	73
Pit 1 Depth (in)	0.15	UTD	NA	UTD	NA	NA	UTD	NA	NA
Pit 2 Depth (in)	0.12	UTD	NA	UT	NA	NA	UTD	NA	NA
Defect P1-23									
Patch Length (in)	3.7	2.3	37	3.8	4	65	3.8	1	60
Patch Width (in)	1.7	1.1	37	1.6	8	44	1.8	5	65
Number of Pits	3.0	2.0		3.0			3.0		
Pit1 Length (in)	0.30	0.40	34	0.52	72	28	0.65	118	62
Pit 2 Length (in)	0.50	Not Seen	NA	0.75	50	NA	0.96	93	NA
Pit 3 Length (in)	0.80	0.49	39	0.75	7	52	1.0	30	113
Pit 1 Width (in)	0.20	0.32	60	0.47	136	48	0.52	159	62
Pit 2 Width (in)	0.60	Not Seen	NA	0.72	20	NA	0.79	31	NA
Pit 3 Width (in)	0.70	0.48	32	0.69	1	45	0.68	3	42
Pit 1 Depth (in)	0.05	0.04	4	UTD	NA	NA	UTD	NA	NA
Pit 2 Depth (in)	0.07	Not Seen	NA	UTD	NA	NA	UTD	NA	NA
Pit 3 Depth (in)	0.09	0.07	13	UTD	NA	NA	UTD	NA	NA

[a]VJ Technologies IXS High Frequency Integrated X-Ray Generator image measurement estimates as determined by the same Mistras staff who interpreted the radiography camera images using VMI StarrView 7 software.
[b] VJ Technologies IXS High Frequency Integrated X-Ray Generator image measurement estimates as determined by the vendor using their ADE software.
NA – Not applicable. This measurement was not determined.
UTD – Unable to determine

Table 7-2. Summary of VJ Technologies IXS High Frequency Integrated X-Ray Generator Percent Error and Percent Difference (% Diff) Results for Defects Not under Insulation

Defect P1-1	Actual	Radiography	% Error	X-ray (Mistras)[a]	% Error	% Diff	X-ray (VJT)[b]	% Error	% Diff
Patch Length (in)	2.0	1.9	6	1.9	5	1	2.0	2	4
Patch Width (in)	1.9	1.9	2	1.9	2	-4	1.9	1	-1
Number of Pits	2.0	2.0		2.0			2.0		
Pit1 Length (in)	0.50	0.34	32	0.37	26	9	0.45	11	31
Pit 2 Length (in)	0.50	0.52	5	0.60	20	14	0.50	1	-5
Pit 1 Width (in)	0.70	0.30	57	0.32	54	5	0.50	29	64
Pit 2 Width (in)	0.40	0.50	24	0.58	45	17	0.38	6	-24
Pit 1 Depth (in)	0.15	UTD	NA	UTD	NA	UTD	UTD	NA	NA
Pit 2 Depth (in)	0.13	UTD	NA	UTD	NA	UTD	UTD	NA	NA
Defect PS 2[c]									
Pit 1 Diameter (in)	0.38	0.36	4	0.39	3	7	0.34	9	-5
Pit 1 Depth (in)	0.19	UTD	NA	UTD	NA	NA	UTD	NA	NA
Pit 2 Diameter (in)	0.31	0.32	1	0.33	4	3	0.30	4	-5
Pit 2 Depth (in)	0.12	UTD	NA	UTD	NA	NA	UTD	NA	NA
Pit 3 Diameter (in)	0.25	0.25	3	0.26	5	8	0.25	2	1
Pit 3 Depth (in)	0.32	UTD	NA	UTD	NA	NA	UTD	NA	NA

[a]VJ Technologies IXS High Frequency Integrated X-Ray Generator image measurement estimates as determined by the same Mistras staff who interpreted the radiography camera images using VMI StarrView 7 software.
[b]VJ Technologies IXS High Frequency Integrated X-Ray Generator image measurement estimates as determined by the vendor using their ADE software.
[c]Pipe Sample 2 simulated defects.
NA – Not applicable. This measurement was not determined.
UTD – Unable to determine

Measurement of all pit lengths and depths from the VJ Technologies IXS High Frequency Integrated X-Ray Generator images were similar across all defects and similar to the average percent errors for the radiography camera, indicating that measurements were able to be obtained from images from both devices with similar accuracy. The average percent error for all patch lengths and widths based on images from the VJ Technologies IXS High Frequency Integrated X-Ray Generator was two to seven times lower than those for the radiography camera. The standard deviations for these average errors were also smaller for the vendor's device, indicating that patch dimensions were more accurately determined using the VJ Technologies IXS High Frequency Integrated X-Ray Generator images.

A variable sensitivity analysis of the methods used to predict the remaining strength of corroded pipe, ASME Standard B31G, shows these assessment criteria are significantly more sensitive to wall thickness than to length or width. The radiography camera was able to assess depth more often (four out of 12 pits) than the VJ Technologies IXS High Frequency Integrated X-Ray

Generator (two out of 12 pits). When both were able measure depth, the radiography camera was 50% more accurate. Depth measurements were not able to be made to the internal pipe wall. The ASME assessment criteria are not as sensitive to errors in length estimations. Length errors that are on the order of a wall thickness or two are typically tolerable. For all length measurements made, the radiography camera had one substantial error while the VJ Technologies IXS High Frequency Integrated X-Ray Generator did not have any. The substantial error observed for the radiography camera was with the shallowest of the four patches tested. Quantification of the edges of shallow corrosion is often difficult, but these anomalies usually do not affect structural performance. The width estimate is the least important parameter in corrosion characterization and is often omitted by the assessment methodologies.

The VJ Technologies IXS High Frequency Integrated X-Ray Generator required the use of a typical 110 V or 220 V power outlet to operate the technology. A connection to a computer was also required to program the x-ray device for taking images and to control the power output. The x-ray tube in the unit has a life span of six to eight years.

The exposure time used for this test was 1 minute. In order to determine an appropriate exposure time and source power, initial images were collected and evaluated until the proper exposure situation was determined. This process took approximately one hour. Preparation of the VJ Technologies IXS High Frequency Integrated X-Ray Generator involved setting it up on a tripod stand and attaching the imaging plate and associated markers and image quality indicators to the pipe and inputting the correct parameters into the software. This process took approximately 10-15 minutes for each image. Similar preparation times were noted for the radiography camera. Positioning the VJ Technologies IXS High Frequency Integrated X-Ray Generator for images above the pipe required the use of a platform to suspend the device the proper distance above the pipe. The x-ray device was placed 28 inches away from the defect (except for the contact image) and was operated at 3 mA and 160 kV. The radiography camera was 32 inches away from the pipe and used an exposure time of 1.5 minutes.

The VJ Technologies IXS High Frequency Integrated X-Ray Generator produces radiation, though not from a radioactive source. Thus, an operator must be properly licensed to safely operate this technology. No maintenance or calibration was needed for the VJ Technologies IXS High Frequency Integrated X-Ray Generator. The technology came factory calibrated and does not need further calibration at any point of its operation. There were no operational issues with the technology during the verification testing.

Significant ghosting was noted on the imaging plates when using this technology. These burned images did not appear to impact the ability of the VJ Technologies IXS High Frequency Integrated X-Ray Generator to take new images or interfere with the interpretation of any images, but they remained on the imaging plates and rendered them useless after the testing was completed. The cost of each phosphor imaging plate was approximately $500.

Chapter 8
References

1. ASTM Standard E-94, "Standard Practice for Radiographic Testing", ASTM International, West Conshohocken, PA, 2009.

2. ISO 5579, "Non-destructive testing – Radiographic examination of metallic materials by X- and gamma-rays – Basic Rules", International Organization for Standardization, Geneva, Switzerland, 1998.

3. BS EN 444, "Non-destructive testing; general principals for the radiographic examination of metallic materials using X-rays and gamma-rays", British Standards Institution, North Hampton, United Kingdom, 1994.

4. *Test/QA Plan for Verification of Alternative Technologies for Sealed Source Radiography Cameras,* Battelle, Columbus, Ohio, May 28, 2010.

5. Environmental Technology Verification Program Quality Management Plan, EPA/600/R-08/009, U.S. Environmental Protection Agency, Cincinnati, Ohio, January 2008.

6. American Petroleum Institute Standard 1163, "In-line Inspection Systems Qualification Standard, Edition 5", API Publications, Englewood, CO, August 2005.

Appendix A

Pipe Sample 1
Defects Characterizations

Metal Loss Corrosion Assessment

Pipe Sample 1, an 8-inch diameter seam-welded pipe measuring approximately 35 feet in length, was used in this verification test. This sample consisted of three pipe sections welded together (two circumferential welds) and contained simulated corrosion defects set along two test lines 180 ° apart. The simulated corrosion was created using electrochemical etching techniques. A five foot section of Pipe Sample 1 also contained natural corrosion from a pipe recently pulled from service.

The donated natural corrosion pipe sample had a field girth weld with corrosion on both sides of the weld. The weld drop through was too large for the inspection tool specifications and as such the pipe was trimmed to include roughly two feet of corrosion on one end, three feet of full thickness pipe at the other end, and no field welds. The pipe was then sandblasted and welded between two new pipes to comprise Pipe Sample 1. When the pipe was being fully characterized, an additional weld was found in the middle of the corrosion area. This weld was very fine and did not have a significant crown.

8-INCH DIAMETER CORROSION DEFECT ASSESSMENT DATA

Detection of Metal Loss - Page 1

Name:	
Date:	
Company:	
Sensor Design:	

CALIBRATION DATA

Pipe Sample	Calibration Metal Loss Location	Metal Loss Length & Width	Depth of Metal Loss	Measured Length & Width of Defect	Measured Max. Depth of Defect	Comments
	inches from End B to center of defect	inches	inches			
PIPE SAMPLE 1:						
Calibration P1-1:	361" (59" from End A)	2 x 2	See profile			

TEST DATA

Pipe Sample:	**PIPE SAMPLE 1**
Defect Set:	8" Diameter, 0.188" Wall Thickness Pipe Sample; Schedule 10; Length = 34' 11.75"

TEST LINE 1

Defect Number	Search Region (Distance from End B)	Start of Metal Loss Region from Side B	End of Metal Loss Region from Side B	Total Length of Metal Loss Region	Width of Metal Loss Region	Maximum Depth of Metal Loss Region	Additional Data Attached?	Comments
	inches	inches	inches	inches	inches	inches	Y/N	
P1-12	52" to 64"	**56.75"**	**60.875"**	**4.125"**	**2"**	**0.122"**	**Y**	**Defect 6**
P1-11	76" to 88"	**---**	**---**	**---**	**---**	**---**	**N**	**BLANK 6**
P1-10	100" to 112"	**---**	**---**	**---**	**---**	**---**	**N**	**BLANK 5**
WELD	120"							
P1-9	120" to 144"	**120"**	**140.25"**	**20.25"**	**Full Circumference**	**0.146"**	**Y**	**P1-NC1**
P1-8	160" to 172"	**---**	**---**	**---**	**---**	**---**	**N**	**BLANK 4 (natural corrosion pipe segment)**
WELD	180"							
P1-7	184" to 196"	**190.625"**	**192.75"**	**2.125"**	**2"**	**0.147"**	**Y**	**Defect 5**
P1-6	208" to 220"	**---**	**---**	**---**	**---**	**---**	**N**	**BLANK 3**
P1-5	232" to 244"	**232.75"**	**235.75"**	**3"**	**1"**	**0.081"**	**Y**	**Defect 4**
P1-4	256" to 268"	**259.625"**	**263.625"**	**4"**	**2"**	**0.063"**	**Y**	**Defect 3**
P1-3	280" to 292"	**287.75"**	**290.875"**	**3.125"**	**2"**	**0.096"**	**Y**	**Defect 2**
P1-2	304" to 316"	**---**	**---**	**---**	**---**	**---**	**N**	**BLANK 2**
P1-1	328" to 340"	**---**	**---**	**---**	**---**	**---**	**N**	**BLANK 1**

TEST LINE 2

Defect Number	Search Region (Distance from End B)	Start of Metal Loss Region from Side B	End of Metal Loss Region from Side B	Total Length of Metal Loss Region	Width of Metal Loss Region	Maximum Depth of Metal Loss Region	Additional Data Attached?	Comments
	inches	inches	inches	inches	inches	inches	Y/N	
P1-23	74" to 86"	**79.75"**	**83.75"**	**4"**	**2"**	**0.097"**	**Y**	**Defect 11**
P1-22	98" to 110"	**108"**	**110"**	**2"**	**2"**	**0.12"**	**Y**	**Defect 10**
WELD	120"							
P1-21	120" to 144"	**120"**	**140.75"**	**20.75"**	**Full Circumference**	**0.127"**	**Y**	**P1-NC2**
P1-20	160" to 172"	**---**	**---**	**---**	**---**	**---**	**N**	**BLANK 11 (natural corrosion pipe segment)**
WELD	180"							
P1-19	186" to 198"	**---**	**---**	**---**	**---**	**---**	**N**	**BLANK 10**
P1-18	210" to 222"	**213.625"**	**217.875"**	**4.25"**	**2"**	**0.145"**	**Y**	**Defect 9**
P1-17	234" to 246"	**---**	**---**	**---**	**---**	**---**	**N**	**BLANK 9**
P1-16	258" to 270"	**---**	**---**	**---**	**---**	**---**	**N**	**BLANK 8**
P1-15	282" to 294"	**---**	**---**	**---**	**---**	**---**	**N**	**BLANK 7**
P1-14	306" to 318"	**308.875"**	**312"**	**3.125"**	**1"**	**0.115"**	**Y**	**Defect 8**
P1-13	330" to 342"	**335.75"**	**339.625"**	**3.875"**	**1.75"**	**0.095"**	**Y**	**Defect 7**

Table A-1. Corrosion Anomalies in 8-inch Diameter Pipe Sample 1

8 INCH PIPE SAMPLE 1 DOCUMENTATION

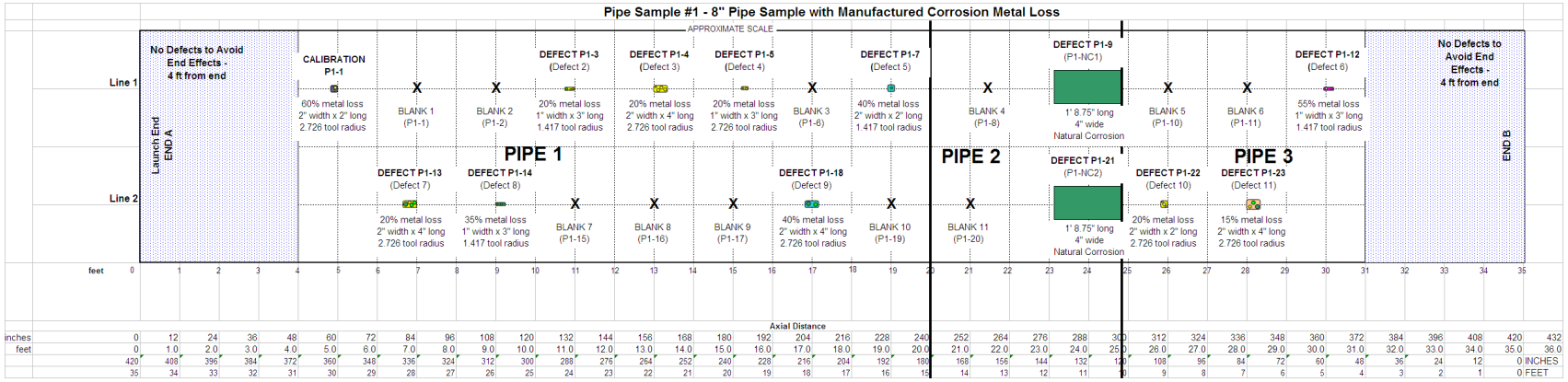

Defect Number	Distance from End A to Defect Center (inches)	Distance from End A to Defect Center (feet)	Length of Defect (in)	Width of Defect (in)	Max Depth of Metal Removed (in)	% Metal Loss	Radius of End Mill Tool
PIPE 1 Line 1							
Calibration P1-1	59.0	4.916667	2	2	0.151	80%	2.726
Blank 1 (P1-1)	84.0	7	-	-	0.00	0%	-
Blank 2 (P1-2)	108.0	9	-	-	0.00	0%	-
Defect P1-3 (Defect 2)	130.5	10.875	3	1	0.096	51%	1.417
Defect P1-4 (Defect 3)	158.0	13.16667	4	2	0.063	34%	2.726
Defect P1-5 (Defect 4)	185.5	15.45833	3	1	0.081	43%	2.726
Blank 3 (P1-6)	204.0	17	-	-	0.00	0%	-
Defect P1-7 (Defect 5)	228.0	19	2	2	0.147	78%	1.417
PIPE 2 Line 1							
Blank 4 (P1-8)	252.0	21	-	-	0.00	0%	-
Defect P1-NC1 (P1-9)	289.5	24.125	20.25	4	0.146	78%	
PIPE 3 Line 1							
Blank 5 (P1-10)	312.0	26	-	-	0.00	0%	-
Blank 6 (P1-11)	336.0	28	-	-	0.00	0%	-
Defect P1-12 (Defect 6)	361.5	30.125	3	1	0.122	65%	1.417
PIPE 1 Line 2							
Defect P1-13 (Defect 7)	82.0	6.833333	4	2	0.095	51%	2.726
Defect P1-14 (Defect 8)	109.5	9.125	3	1	0.115	61%	1.417
Blank 7 (P1-15)	132.0	11	-	-	0.00	0%	-
Blank 8 (P1-16)	156.0	13	-	-	0.00	0%	-
Blank 9 (P1-17)	180.0	15	-	-	0.00	0%	-
Defect P1-18 (Defect 9)	204.0	17	4	2	0.145	77%	2.726
Blank 10 (P1-19)	228.0	19	-	-	0.00	0%	-
PIPE 2 Line 2							
Blank 10 (P1-20)	252.0	21	-	-	0.00	0%	2.726
Defect P1-NC2 (P1-21)	289.0	24.08333	20.75	4	0.127	68%	
PIPE 3 Line 2							
Defect P1-22 (Defect 10)	311.0	25.91667	2	2	0.120	64%	2.726
Defect P1-23 (Defect 11)	338.0	28.16667	4	2	0.097	52%	2.726

Figure A-1. 8-inch Pipe Sample 1 Defect Map

Pipe Sample 1 Simulated Corrosion Defect Photos

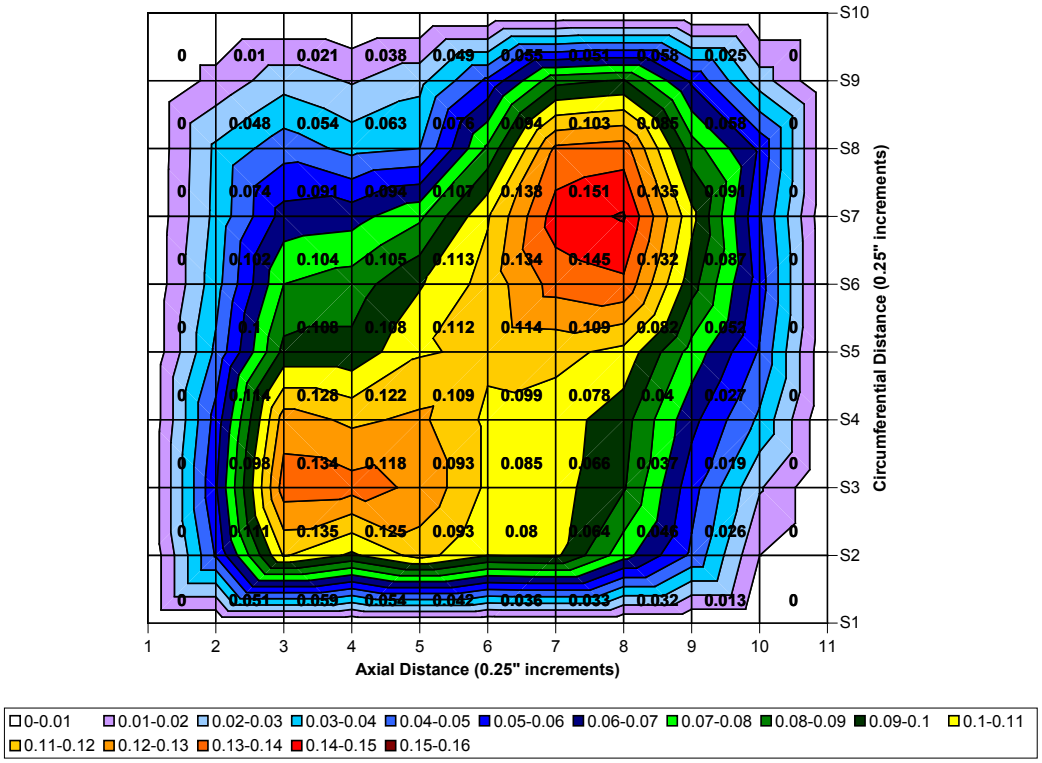

Figure A-2. Defect P1-1 (Defect 1)

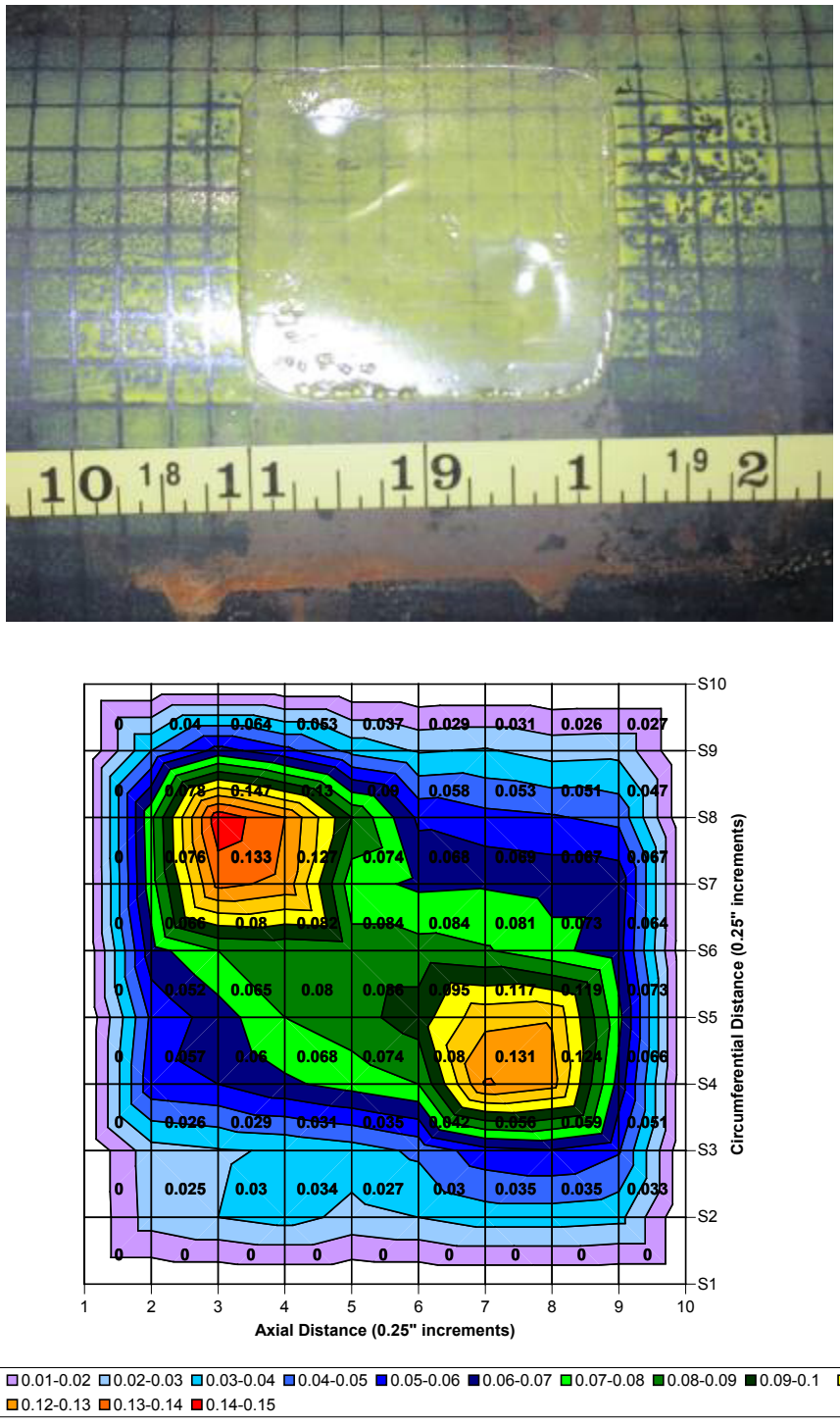

Figure A-3. Defect P1-7 (Defect 5)

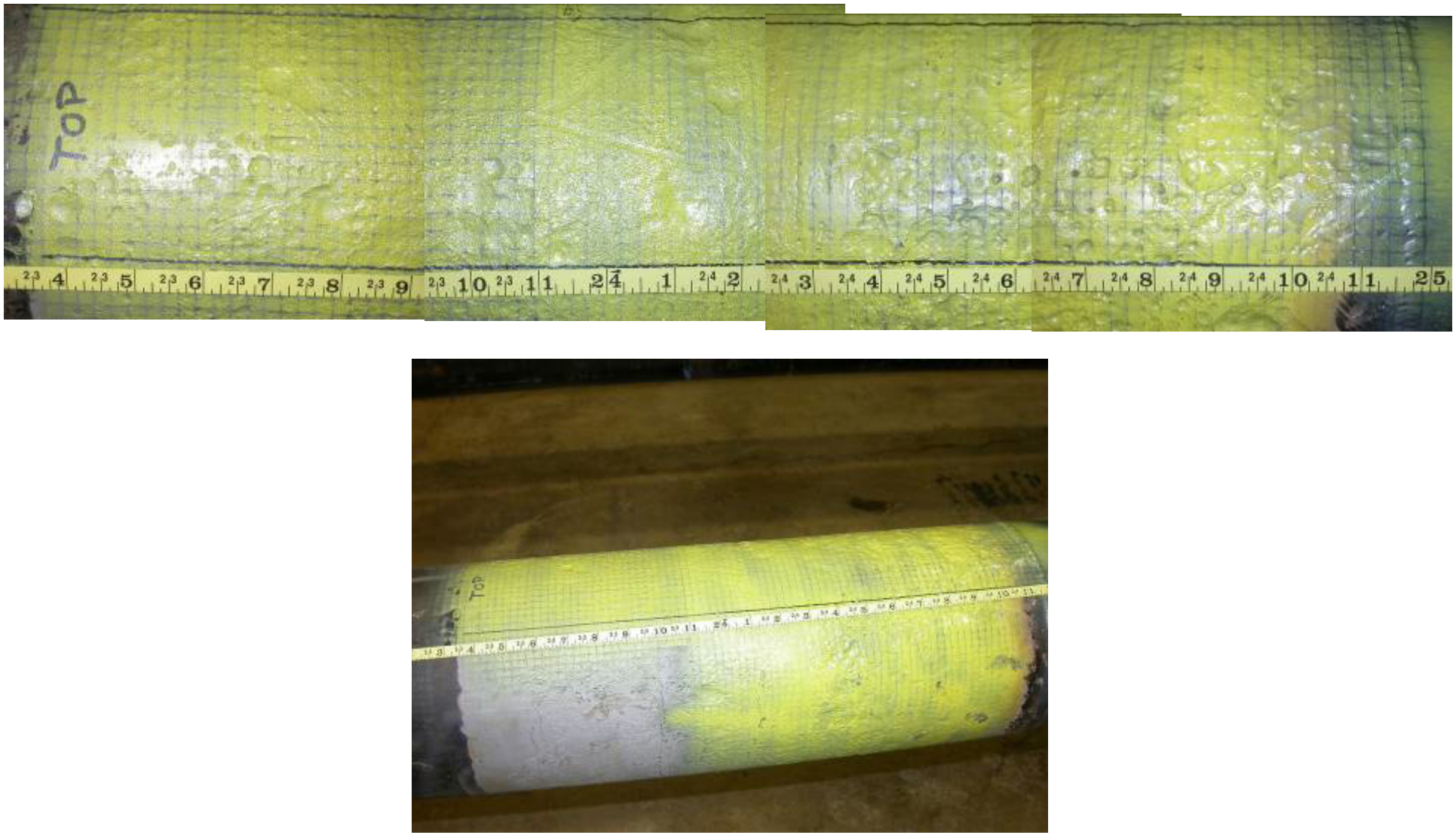

Figure A-4. Defect P1-9 (P1-NC1)

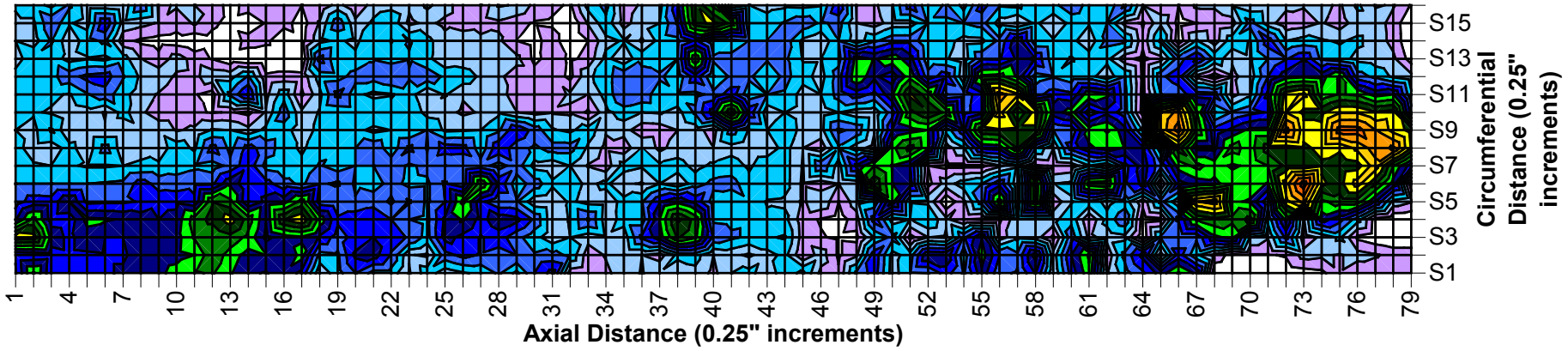

Figure A-4 (cont). Defect P1-9 (P1-NC1)

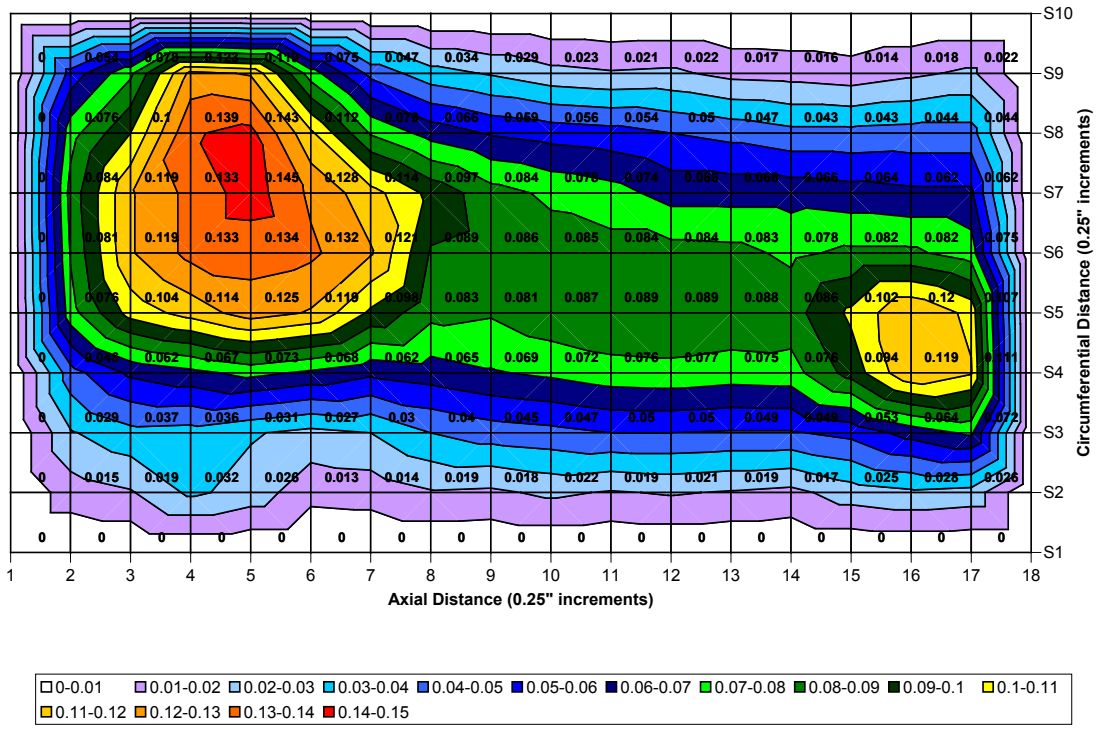

Figure A-5. Defect P1-18 (Defect 9)

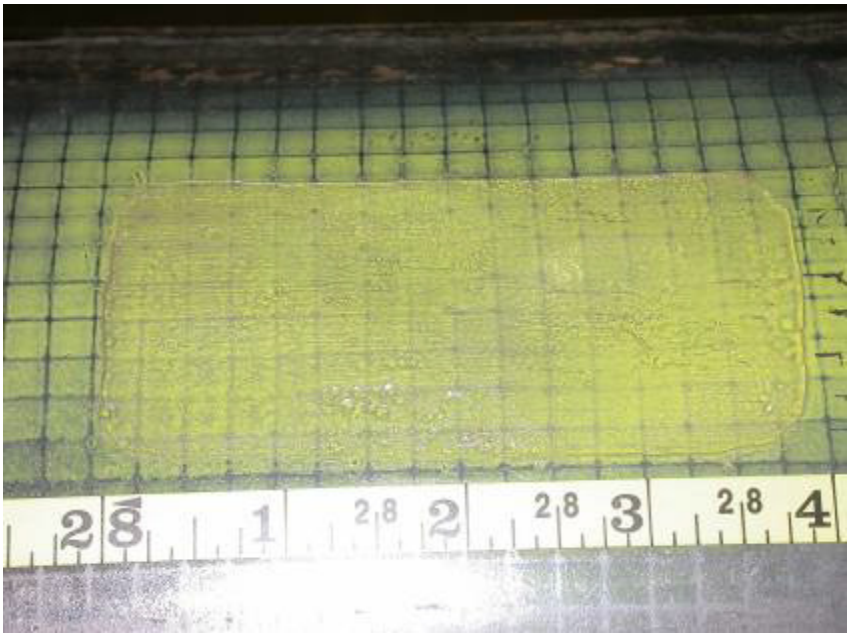

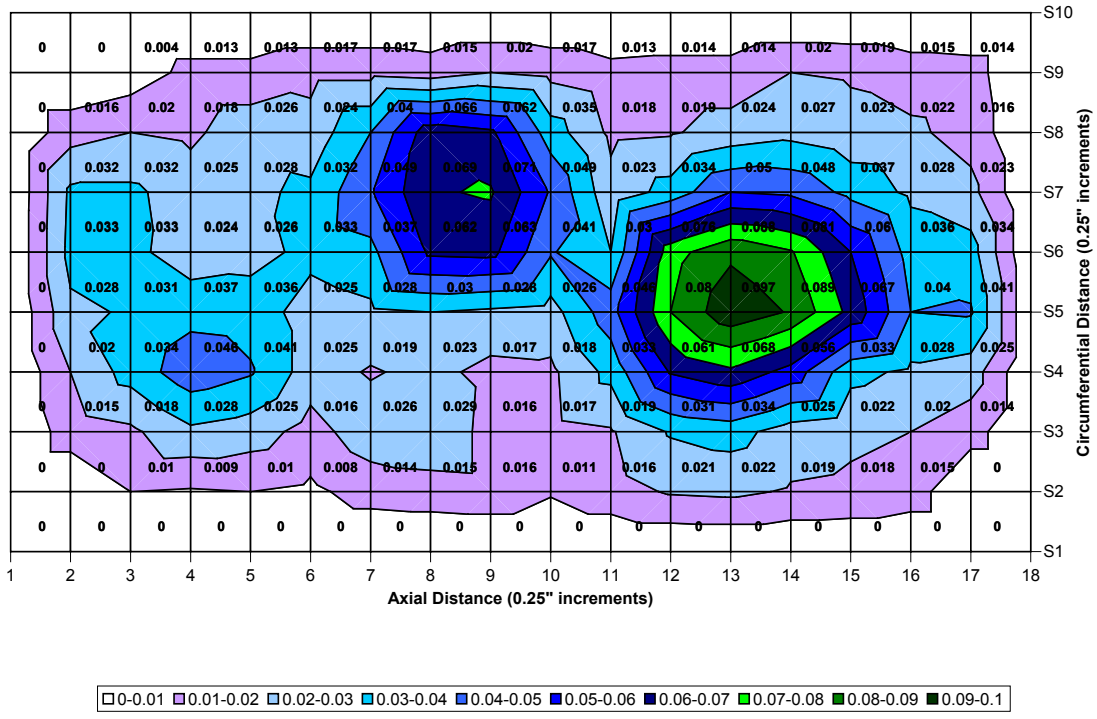

Figure A-6. Defect P1-23 (Defect 1)